PERFORMANCE EVALUATION OF UWB-IR SYSTEM

A DISSERTATION

Submitted in partial fulfillment of the requirements for the award of the degree of

MASTER OF TECHNOLOGY

in

ELECTRONICS AND COMPUTER ENGINEERING

(With Specialization in Communication Systems)

By

JITU SANWALE

DEPARTMENT OF ELECTRONICS AND COMPUTER ENGINEERING
INDIAN INSTITUTE OF TECHNOLOGY ROORKEE
ROORKEE -247 667 (INDIA)

JUNE, 2008

CANDIDATE'S DECLARATION

I hereby declare that the work, which is presented in this dissertation report entitled, **"PERFORMANCE EVALUATION OF UWB-IR SYSTEM"** towards the partial fulfillment of the requirements for the award of the degree of **Master of Technology** with specialization in **Communication Systems**, submitted in the Department of Electronics and Computer Engineering, Indian Institute of Technology Roorkee, Roorkee (India) is an authentic record of my own work carried out during the period from July 2007 to June 2008, under the guidance of **Dr. A. TYAGI, Assistant Professor, Department of Electronics and Computer Engineering, Indian Institute of Technology Roorkee.**

I have not submitted the matter embodied in this dissertation for the award of any other Degree or Diploma.

Date:

Place: Roorkee

JITU SANWALE

CERTIFICATE

This is to certify that the above statement made by the candidate is correct to the best of my knowledge and belief.

Date:

Place: Roorkee

Dr. A. TYAGI,
Assistant Professor, E&C Department,
IIT Roorkee,
Roorkee – 247 667 (India).

ACKNOWLEDGMENTS

My greatest debt is to my thesis supervisor **Dr. Anshul Tyagi** for his guidance, suggestions, encouragement and support. I am so greatful to him for leading me into this exciting research area. I also express my great thanks to **Mr. S. Chakravorty**, for being a good teacher. His course on Wireless Networks has well prepared me for carrying out this thesis work. I like to thank **Dr. D. K. Mehra** and all teaching staff for their kind support and encouragement throughout the course.

I feel fortunate to work with my colleagues. I also express my gratitude to Anand and both Gauravs for being good friends and all their helps in these two years. I thank Kishore, Anil, DJ and other people who have combined to create a good working place.

I owe special thanks to my parents, for their support and encouragement in my everyday's life. I extend hearty thanks to my younger brother Dipak and my best friends Vivek and Piyush for their constant motivation.

I extend my gratitude to Mr. Narad Singh Sarel, Mrs. Sarel, Ankit and Anshita for their support and encouragement.

Finally, I show my deepest gratitude to God for everything which, he has done for me and for his blessings.

JITU SANWALE

ABSTRACT

Ultra Wideband Technology for commercial communication application is a recent innovation. Short-range wireless systems have recently gained a lot of attention to provide multimedia communications and to run high speed applications around a user centric concept in so called Wireless Personal Area Networks (WPAN). UWB technology presents itself as a good candidate for the physical layer of the WPAN.

In this thesis, we present a comparative study analysis and system performances of the time-hopping and direct-sequence systems. TH-PPM is a originally proposed modulation scheme for UWB systems. We have shown the bit error rate (BER) performance of the TH-PPM, TH-BPSK, DS-PPM and DS-BPSK systems.

Further, we extended our work for different number of users and different monocycles used for the transmission. Under different system parameters, the BER of time-hopping and direct-sequence systems are examined.

CONTENTS

FIGURES

Chapter 1

INTRODUCTION

1.1 Introduction

Today's emerging technology Ultra-wideband impulse radio (UWB-IR) is built on a long history of technological advancements in the field of wireless communication. Since the invention of first wireless telephone system by Marconi, a steep growth is seen in wireless services. The number of cellular phone users has increased dramatically. With the rapid proliferation of wireless communication services in past decades, the wireless technology also has grown enormously.

UWB-IR is a most recent technology in wireless communications. It has received great attention in both academia and industry for applications in wireless communications. However, it is as deeply rooted as wireless communication itself. UWB-IR is a fast emerging technology with uniquely attractive features inviting major advances in wireless communications, networking, radar, imaging and positioning systems.

1.2 UWB Communication System

UWB-IR is based on the continuous transmission of very short pulses; very short refers to pulse duration of the order of nano seconds. The information bits are usually transferred by one or more pulses.

The Federal Communications Commission (FCC) has allocated 7.5 GHz of the spectrum for unlicensed use of UWB devices in the 3.1 to10.6 GHz frequency band. A UWB system is defined as any radio system that has a 10-dB bandwidth larger than 25 percent of its center frequency, or has a 10-dB bandwidth equal to or larger than 1.5 GHz if the center frequency is greater than 6 GHz, that is $B > \frac{f_c}{4}$, where $B = f_H - f_L$ and

$f_c = \frac{f_H + f_L}{2}$ with f_H and f_L are being the upper and lower 10-dB cut off points respectively.

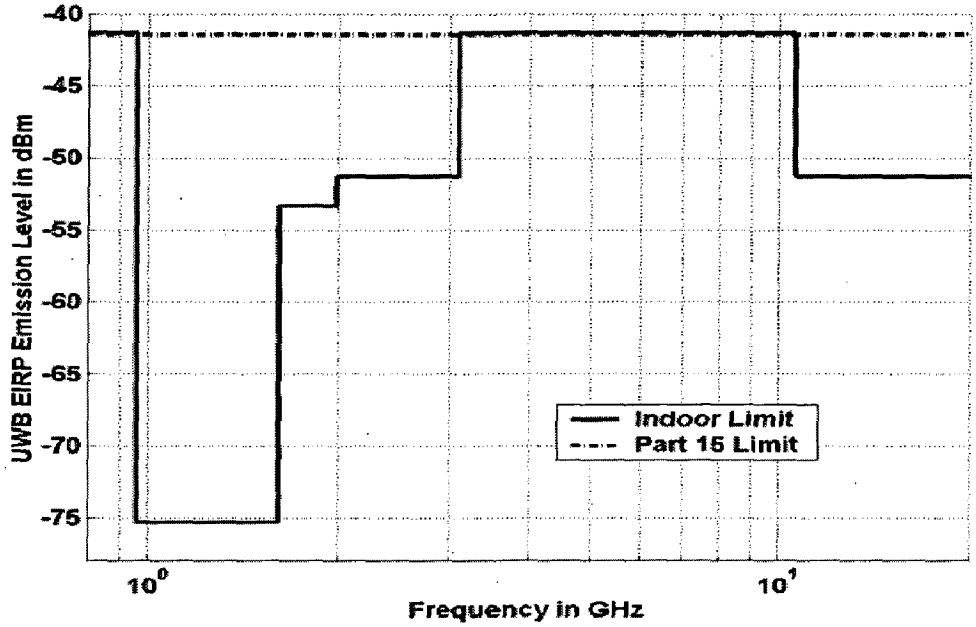

Fig 1.1 FCC Spectral Masks for UWB Indoor Communications Systems [1]

In general, UWB technology has many benefits due to its ultra-wideband nature which include high data rate, less path loss and better immunity to multipath propagation, availability of low-cost transceivers due to absence of carrier signal and extremely low power spectral density (PSD). The applications majorly cover two areas namely location and communication. Locations include ranging instruments; ground penetration radars for mine detection, tracking and precision location; military, public safety and rescue teams application. Broad-band ad-hoc wireless networks; Local Area Networks (LANs); Body Area Networks (BANs); smart-home systems; fourth generation cellular systems comes under the category of communication applications.

1.3 UWB Transmission

UWB usually refers to impulse based waveforms that can be used with different modulation schemes. The transmitted signal consists of a train of very narrow pulses at base band, normally of the order of a nano– seconds. Each transmitted pulse is referred to

as a monocycle. The information can be carried by the position or amplitude of the pulses.

1.3.1 Monocycle Waveforms [2]

The frequency-domain spectral content of a UWB signal depends on the pulse waveform shape and the pulse width. Typical pulse waveforms used in research include:

- Rectangular,
- Gaussian,
- Gaussian doublet, and
- Rayleigh monocycles, etc.

A monocycle should have zero DC components to allow it to radiate effectively.

A rectangular monocycle with width T_p can be represented by $\left[u(t)-u(t-T_p)\right]$, where $u(.)$ denotes the unit step function. The rectangular pulse has a large DC component, which is not a desired property.

In most of the cases for communication purpose Gaussian pulses and it's derivatives are used. The reason behind the popularity of these pulses is twofold: i) Gaussian pulses come with the smallest possible time-bandwidth product of 0.5, which maximizes range-rate resolution, and ii) The Gaussian pulses are readily available from the antenna pattern. A generic Gaussian pulse is given by

$$p_g(t)=\frac{1}{\sqrt{2\pi}\sigma}e^{-\frac{1}{2}\left(\frac{t-\mu}{\sigma}\right)^2} \tag{1.1}$$

Where μ defines the center of the pulse and σ determines the width of the pulse. Some monocycles are derived from the Gaussian pulse. The Gaussian monocycle is the second derivative of a Gaussian pulse, and is given by

$$p_G(t)=A_G\left[1-\left(\frac{t-\mu}{\sigma}\right)^2\right]e^{-\frac{1}{2}\left(\frac{t-\mu}{\sigma}\right)^2} \tag{1.2}$$

Where the parameter σ determines the monocycle width. The effective time duration of the waveform that contains 99.99% of the total monocycle energy is $T_p=7\sigma$ centered at $\mu=3.5\sigma$. The factor A_G introduced so that the total energy of the monocycle is normalized to unity.

The Rayleigh monocycle is derived from the first derivative of the Gaussian pulse and is given by

$$p_R(t) = A_R\left[\frac{t-\mu}{\sigma^2}\right]e^{-\frac{1}{2}\left(\frac{t-\mu}{\sigma}\right)^2} \tag{1.3}$$

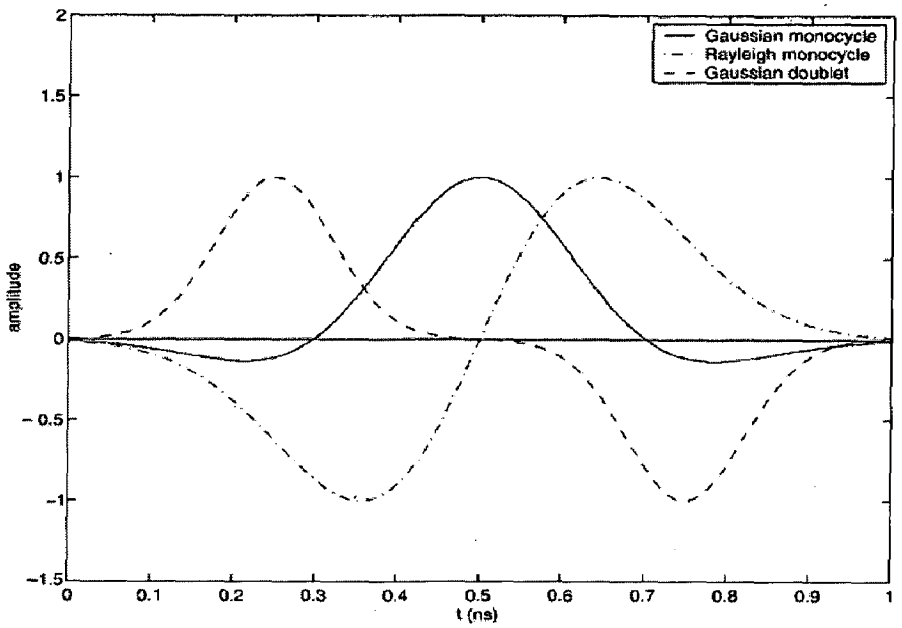

Fig 1.2 The monocycle waveforms

Different from the rectangular waveform, an important feature of the above monocycle is that they do not have a DC component, which makes the radiation of the monocycles more efficient.

Define the -10 dB bandwidth of the monocycles as $B_{10dB} = f_H - f_L$, where f_H and f_L are the frequencies at which the magnitude spectrum attains $1/\sqrt{10}$ of its peak value, and the nominal center frequency as $f_c = \frac{f_H + f_L}{2}$.

1.3.2 Criteria

Important criteria in designing the monocycle waveform include:

1. Simplicity of the monocycle generator, and
2. Minimal interference between the UWB system and other narrowband system coexisting in the same frequency band .

1.3.3 Channel modeling [3]

In 1987 Saleh-Valenzuala gave a channel model based on measurements utilizing low power Ultra-short pulses of width 10ns and center frequency 1.5GHz in medium-size, two storey building. In this model he assumed that, mutipath components arrive at the receiver in groups (clusters) .The arrival of these clusters are assumed to be Poisson distributed with rate Λ. Within each cluster, the arrival of the multipath components are also assumed to be Poisson distributed with rate $\lambda > \Lambda$. In this modeling, the channel impulse response is given by-

$$h(t) = \sum_{l=0}^{\infty} \alpha_l \delta(t - \tau_l)$$

$$= \sum_{m=0}^{\infty} \sum_{n=0}^{\infty} \alpha_{m,n} e^{j\theta_{m,n}} \delta(t - T_m - \tau_{m,n}) \qquad (1.4)$$

$\alpha_{m,n}$ denotes the gain of the n^{th} multipath component of the m^{th} cluster, having phase $\theta_{m,n}$. $T_m + \tau_{m,n} (\tau_{m,0} = 0)$ denotes the arrival time of the n^{th} component of the m^{th} cluster, $\theta_{m,n}$ are independent uniform random variable over [0 2π] and $\alpha_{m,n}$ are independent Rayleigh random variable.

In 2002, the channel modeling subcommittee of the IEEE 802.15.3a Task group recommended a channel model, which includes aforementioned work as well as recent advancements. According to this new model which is nothing but modified version of Saleh-Valenzuala model, the total number of paths is defined as the number of multi-path arrivals with expected power within 10dB from that of the strongest arrival. In this model Rayleigh distributed model parameter α_l is replaced by log-normal distribution. The phase $\theta_{m,n}$ are also constrained to take values 0 or π, with equal probability to account for signal inversion due to reflection, yielding a real valued channel model.

Let $p(t)$ denote the transmitted pulse of duration T_p. After multipath propagation the received waveform $g(t)$ is given by

$$g(t) = p(t) \otimes h(t)$$

$$= \sum_{l=0}^{L} \alpha_l p(t - \tau_l)$$

$$= \sum_{m=0}^{\infty} \sum_{n=0}^{\infty} \alpha_{m,n} e^{j\theta m,n} p(t - T_m - \tau_{m,n}) \quad (1.5)$$

Where $\otimes$ denotes the convolution

The spacing among multipath delays $\{\tau_l\}_{l=0}^{L}$ is in the order of nano seconds. These delayed copies of $p(t)$ can be resolved in $g(t)$ if T_p is sufficiently small.

1.4 Modulation [4]

We define two basic types of modulation for UWB Communications. These are:

- Time based techniques
    1. Pulse position modulation (PPM)
- Shape-based techniques
    1. Bi-phase modulation (BPM)
    2. On-off keying (OOK)
    3. Pulse amplitude modulation (PAM)
    4. General pulse shape modulation (e.g. orthogonal pulse modulation, OPM).

1.4.1 Pulse Position Modulation(PPM)

An important parameter in the pulse position modulation is the delay of the pulse. That is, by defining an arbitrary shape $p(t)$, we can modulate the data by the delay parameter $\tau_i \in \{0, \delta\}$ to create pulses s_i , as

$$s_i = p(t - \tau_i) \quad (1.6)$$

Where $i = 1, 2$ and s_1, s_2 represent transmitted signals for information bits 0 and 1. The advantage of PPM is that it is simple and the ease with which the delay can be controlled.

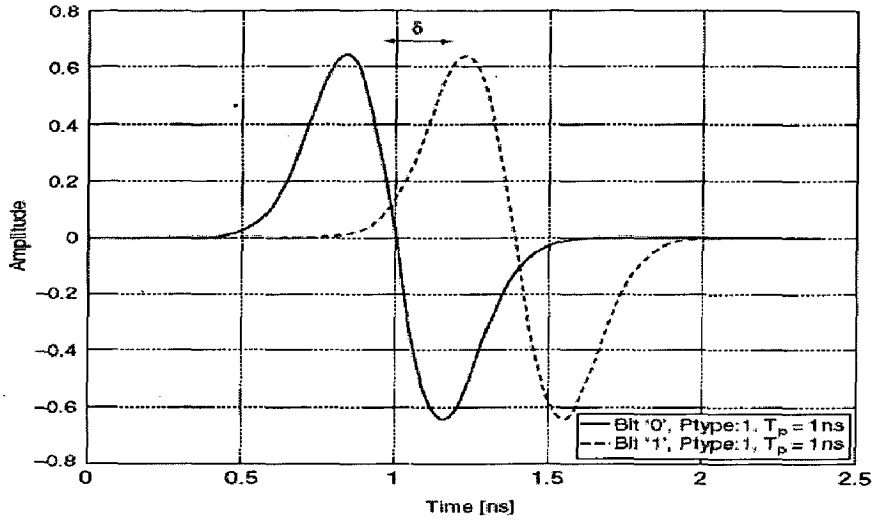

Fig 1.3 PPM waveforms

1.4.2 Bi-phase modulation(BPM)

Mathematical representation for the BPM is stated as:

$$s_i = \sigma_i p(t) \tag{1.7}$$

where $\sigma_i \in \{1, -1\}$

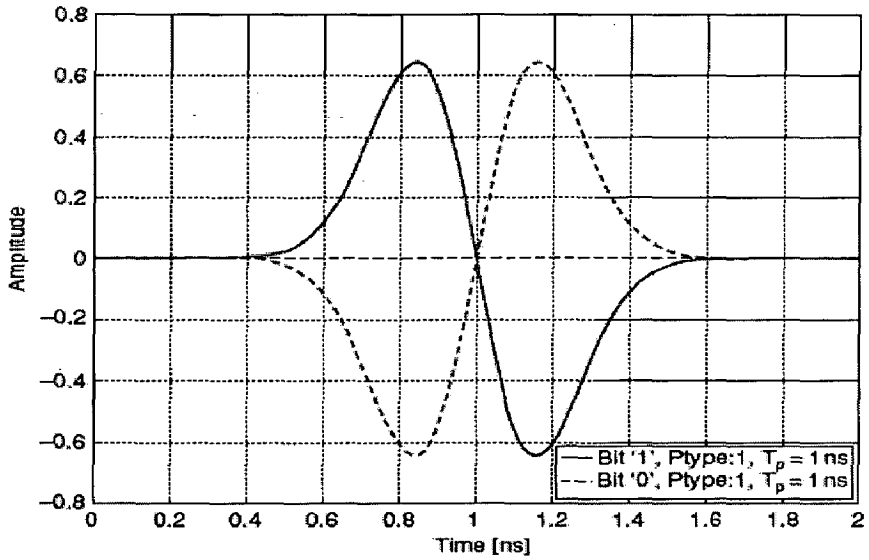

Fig 1.4 BPM waveforms

The parameter σ is known as the shape parameter. For a binary system two resultant pulse shapes s_1 and s_2 are defined simply as $s_1 = p(t)$ and $s_2 = -p(t)$.

1.4.3 Pulse-amplitude modulation (PAM)

Pulse-amplitude modulation (PAM) for UWB can be represented as

$$s_i = \sigma_i p(t) \ , \qquad \sigma_i > 0$$

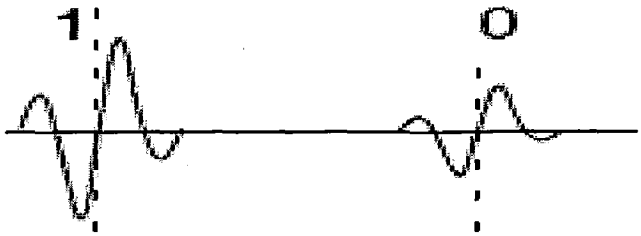

Fig 1.5 PAM waveforms

Where the pulse shape parameter σ takes on positive values greater than zero. For example, in binary system $\sigma_i \in \{1,2\}$ and $s_1 = p(t)$, $s_2 = 2p(t)$.

In general PAM is not preferred for most short range communication. The reason is, an amplitude modulated signal which has smaller amplitude is more susceptible to noise interference than larger counterpart. Furthermore, more power is required to transmit the higher amplitude pulse.

1.4.4 On-Off Keying (OOK)

On-off keying (OOK) for UWB can be characterized as a type of pulse shape modulation where the shape parameter σ is either 0 or 1 and transmitted signal represented as

$$s_i = \sigma_i p(t) \qquad \sigma_i \in \{0,1\}$$

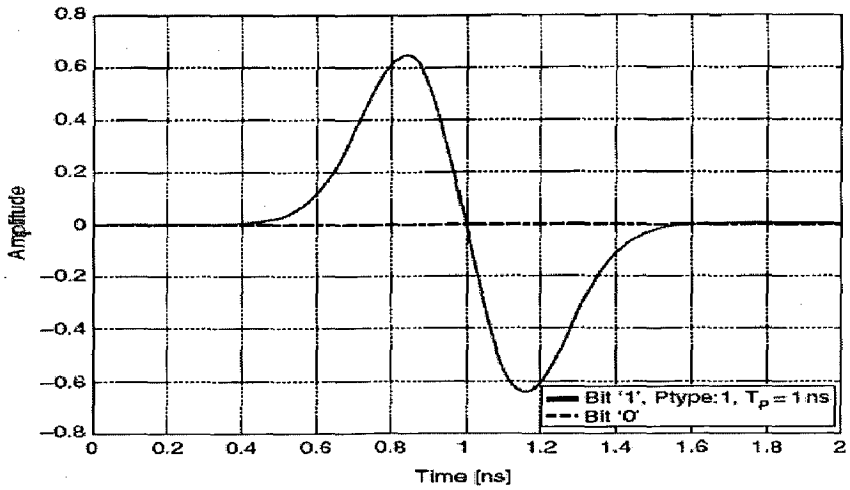

Fig 1.6 OOK waveforms

The problem in OOK is the presence of multipath, in which echoes of the original or other pulses make it difficult to determine the absence of a pulse. It is a binary modulation. It can't be extended to M-ary modulation, as can PPM, PAM and OPM.

Although OOK has a very straightforward implementation, there are numerous system drawbacks. In either, in hardware or software based receiver design, synchronization can be easily lost if the data contains a steady stream of '0's. Also, the BER performance of OOK is worse than bi-phase modulation due to the smaller symbol separation for equal symbol energy.

1.4.5 Orthogonal – Pulse Modulation (OPM)

Orthogonal-pulse modulation (OPM) is simply a subset of general pulse shape modulation with the property that the pulse shapes are orthogonal to each other. The advantage of OPM is not strictly related to the modulation, rather to the multiple access method. Unfortunately, a simple pulse shape parameter σ is inadequate to describe the set of pulses which we may encounter, and here we simply label each pulse as a general $p_1, p_2, \ldots\ldots\ldots p_i$ and assume that pulses are designed so as to be orthogonal.

$$s_i = \{p_1, p_2, \ldots\ldots\ldots p_i\} \tag{1.8}$$

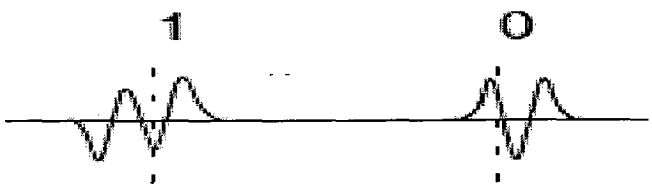

Fig 1.7 OPM waveforms

1.5 Multiple Access [12]

Multiple access (MA) in UWB communication is an area of active research. To date several time-division or code-division pulse amplitude modulation (PAM) or pulse position modulation (PPM) schemes have been proposed to separate multiple users in UWB communications. Conventionally, all users employ the same pulse shape and modulate the transmit pulse based on changing amplitude or position. One concern with using the same pulse for all channels is that the multiple access interference (MAI)

increases as the number of users increase. This is due to increased cross-correlation between similar pulses of the different channels, raising thus the noise floor in such systems.

1.5.1 Time Hopping UWB

Multiple access is achieved in impulse radio through timely sharing the channel. From [8], time hopping sequence must have a distinct time shift pattern assigned to each user in order to eliminate catastrophic collisions.

i) *Uniform Pulse Train Spacing:* A pulse train of the form $s(t) = \sum_{j=-\infty}^{+\infty} w(t - jT_f)$ consists of monocycle pulses spaced T_f seconds apart in time. The frame or pulse repetition time typically may be a hundred to a thousand times the monocycle width, resulting in a signal with a very low duty cycle. Fig1.8 shows the relationship between T_f and T_p.

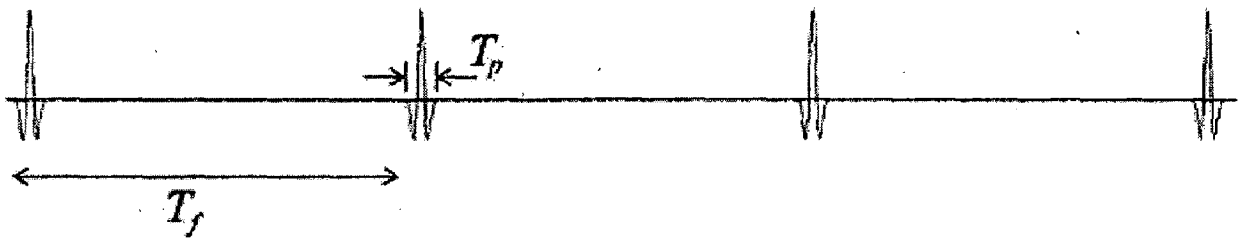

Fig.1.8 Relationship between T_f and T_p.

ii) Random/Pseudorandom TH: In this scheme, each user is assigned a distinct pulse-shift pattern $c_j^{(k)}$, called a TH sequence. For UWB systems, spreading properties of time hopping codes are discussed in [11]. These time hopping sequences $c_j^{(k)}$ are pseudorandom with period N_h and $c_j^{(k)} \in (0, N_h - 1)$.

As defined in [4] and [8], the modulating data is assumed to change only every N_s. Fig.1.9 shows the repetition structure where bit duration $T_b = N_s T_f$.

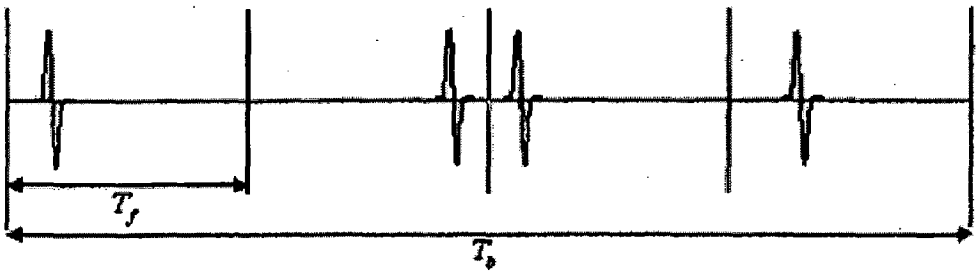

Fig.1.9 The repetition structure of the information bit

iii) Modulation Schemes: An information bit is spread over multiple pulses to achieve a processing due to the repetition structure.

The information signal $s(t)$ for the k^{th} user can be written as

$$s^{(k)}(t) = \sum_{i=-\infty}^{\infty} \sum_{j=0}^{N_s-1} p(t - iT_b - jT_f - c_j^{(k)} T_c) d_i^{(k)}$$

For PAM modulation

$$s^{(k)}(t) = \sum_{i=-\infty}^{\infty} \sum_{j=0}^{N_s-1} p(t - iT_b - jT_f - c_j^{(k)} T_c - \delta d_i^{(k)})$$

For PPM modulation

$$s^{(k)}(t) = \sum_{i=-\infty}^{\infty} \sum_{j=0}^{N_s-1} p_{d_i^{(k)}}(t - iT_b - jT_f - c_j^{(k)} T_c)$$

For PSM modulation

1.5.2 Direct Sequence UWB

In direct-sequence UWB systems, a pseudo random code is used to spread an information bit into chips. Performance of DS systems is discussed in [19] and [21]. In a typical direct-sequence spreading scheme, the binary base band pulse amplitude modulated signal for k^{th} user is given as

$$s^{(k)}(t) = \sum_{i=-\infty}^{\infty} \sum_{j=0}^{N_s-1} d_i^{(k)} c_j^{(k)} p(t - iT_b - jT_c)$$

Where $c_j^{(k)}$ is a direct-sequence for the k^{th} user and takes values $c_j^{(k)} \in \{-1, +1\}$. Pseudo-random codes are used to separate users and to provide a processing gain.

The remainder of the chapter is organized as follows. In section 2.2, system models for different modulation schemes (i.e. TH-PPM, TH-BPSK) are presented. Analysis of various modulation schemes is done in section 2.3 and 2.4, section 2.5 is fully devoted in deriving BER expressions for TH-PPM and TH-BPSK systems. Finally, simulation results and comparison of TH-PPM and TH-BPSK for different values of parameters are summarized in section 2.6 and 2.7.

2.2 System Model

We consider a UWB communication system described in [6], [8], [10] and [13], in which each user is assigned a unique and random time hopping code $c^{(k)}$, where $0 \le c^{(k)} < N_h$. This spreading code is basically used to randomize the transmitted pulse timing instants by T_c and is designed in such a way that $N_h T_c \le T_f$.

In UWB systems, the choice of transmitting pulse strongly affects the bit error rate performance. There are number of pulses, proposed for UWB communications including the Gaussian pulse, derivatives of Gaussian pulse, Manchester monocycle and Hermite pulses. For this system, we have used doubly differentiated Gaussian pulse given below (also shown in fig.2.1)

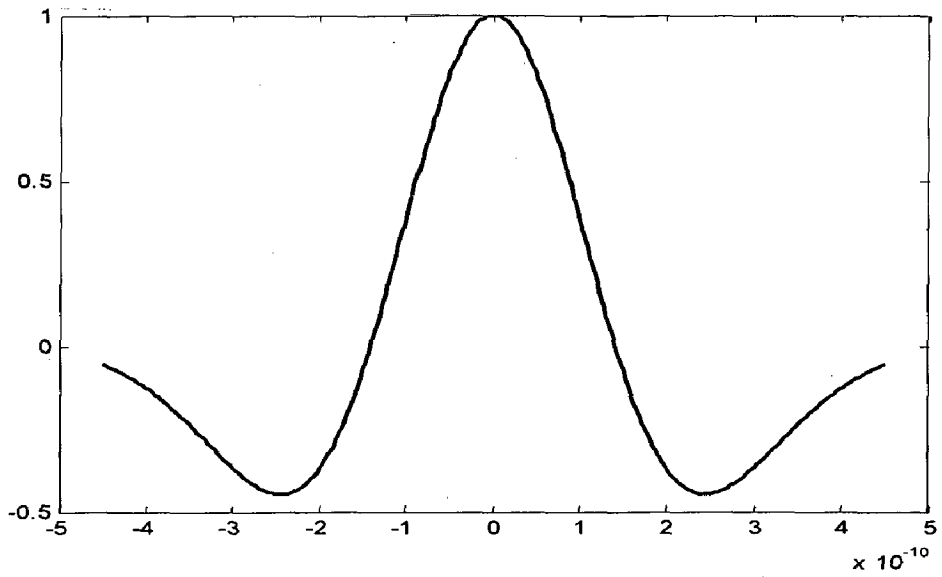

Fig.2.1 Doubly differentiated Gaussian pulse

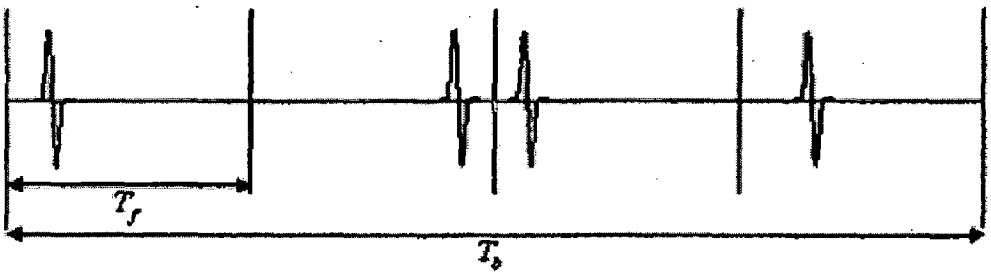

Fig.1.9 The repetition structure of the information bit

iii) Modulation Schemes: An information bit is spread over multiple pulses to achieve a processing due to the repetition structure.

The information signal $s(t)$ for the k^{th} user can be written as

$$s^{(k)}(t) = \sum_{i=-\infty}^{\infty} \sum_{j=0}^{N_s-1} p(t - iT_b - jT_f - c_j^{(k)} T_c) d_i^{(k)}$$

For PAM modulation

$$s^{(k)}(t) = \sum_{i=-\infty}^{\infty} \sum_{j=0}^{N_s-1} p(t - iT_b - jT_f - c_j^{(k)} T_c - \delta d_i^{(k)})$$

For PPM modulation

$$s^{(k)}(t) = \sum_{i=-\infty}^{\infty} \sum_{j=0}^{N_s-1} p_{d_i^{(k)}}(t - iT_b - jT_f - c_j^{(k)} T_c)$$

For PSM modulation

1.5.2 Direct Sequence UWB

In direct-sequence UWB systems, a pseudo random code is used to spread an information bit into chips. Performance of DS systems is discussed in [19] and [21]. In a typical direct-sequence spreading scheme, the binary base band pulse amplitude modulated signal for k^{th} user is given as

$$s^{(k)}(t) = \sum_{i=-\infty}^{\infty} \sum_{j=0}^{N_s-1} d_i^{(k)} c_j^{(k)} p(t - iT_b - jT_c)$$

Where $c_j^{(k)}$ is a direct-sequence for the k^{th} user and takes values $c_j^{(k)} \in \{-1, +1\}$. Pseudo-random codes are used to separate users and to provide a processing gain.

Chapter 2

Performance Evaluation of Multiple Access in TH-PPM and TH-BPSK UWB-IR Systems

2.1 Introduction

Ultra-wideband (UWB) technology has been recently proposed as a viable candidate for short range wireless communication systems. And the reason is, it's robustness against multipath. Ultra wide bandwidth makes UWB attractive for multiple access applications. Initially, time hopped pulse position modulation was proposed as a system model for UWB technology. Time hopping concept in UWB systems is basically used to eliminate catastrophic collisions in multiple access.

The bit error rate (BER) of TH-PPM system in presence of multiple access interference in AWGN channel is studied in [5] and [6]. In this study, they have modeled multi user interference (MUI) as a Gaussian approximation or "standard approximation" and Gaussian quadrature rules (GQR) respectively. In Gaussian approximation approach, a central limit theorem (CLT) is employed to approximate the multiple access interference as an additive white Gaussian process. In most of the cases Gaussian approach is used to evaluate the performance, because it is easy to apply. However, it is shown in [4], [13] and [14] that, this underestimates the performance of the system in terms of BER at higher values of signal to noise ratio (SNR). The limitation of Gaussian approximation encouraged researchers to find better ways to evaluate BER. In [5], a simulation based semi-analytical estimate is formed using results from a Gaussian quadrature rule approximation of a definite integral.

It is unwieldy to derive an exact expression for BER for asynchronous multiple access UWB system. In [9], [10], [11] and [13], precise bit error rate is calculated for TH-PPM and TH-BPSK. They have provided expressions for the characteristic functions of the multi access interference (MAI) in different modulation schemes.

In this chapter, we analyze TH-PPM and TH-BPSK systems in multiple access interference for additive white Gaussian noise channel.

The remainder of the chapter is organized as follows. In section 2.2, system models for different modulation schemes (i.e. TH-PPM, TH-BPSK) are presented. Analysis of various modulation schemes is done in section 2.3 and 2.4, section 2.5 is fully devoted in deriving BER expressions for TH-PPM and TH-BPSK systems. Finally, simulation results and comparison of TH-PPM and TH-BPSK for different values of parameters are summarized in section 2.6 and 2.7.

2.2 System Model

We consider a UWB communication system described in [6], [8], [10] and [13], in which each user is assigned a unique and random time hopping code $c^{(k)}$, where $0 \leq c^{(k)} < N_h$. This spreading code is basically used to randomize the transmitted pulse timing instants by T_c and is designed in such a way that $N_h T_c \leq T_f$.

In UWB systems, the choice of transmitting pulse strongly affects the bit error rate performance. There are number of pulses, proposed for UWB communications including the Gaussian pulse, derivatives of Gaussian pulse, Manchester monocycle and Hermite pulses. For this system, we have used doubly differentiated Gaussian pulse given below (also shown in fig.2.1)

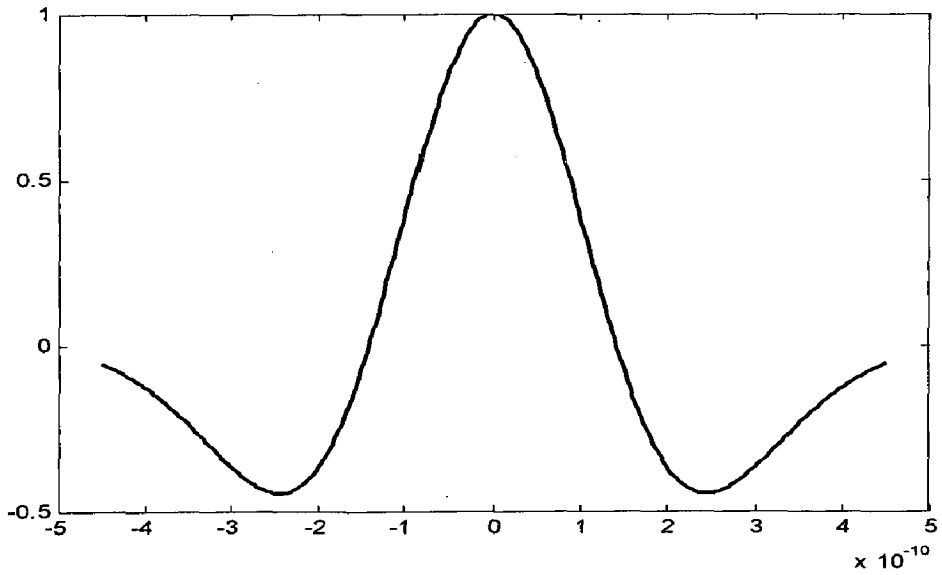

Fig.2.1 Doubly differentiated Gaussian pulse

$$p(t)=\left[1-4\pi\left(\frac{t}{\tau_p}\right)^2\right]\exp\left[-2\pi\left(\frac{t}{\tau_p}\right)^2\right] \tag{2.1}$$

Where τ_p represents a time normalizing factor which determines the width of the pulse. In this work, we have compared the bit error rate performance by using Gaussian pulse and doubly differentiated Gaussian pulse or 2nd- order Gaussian pulse. The Gaussian pulse is represented by

$$p_g(t)=\exp\left[-2\pi\left(\frac{t}{\tau_p}\right)^2\right] \tag{2.2}$$

The signaling waveform of TH-PPM UWB system for the k^{th} user is given by

$$s^{(k)}(t,i)=\sqrt{\frac{E_b}{N_s}}\sum_{j=iN_s}^{(i+1)N_s-1}p(t-jT_f-c_j^{(k)}T_c-d_i^{(k)}\delta) \tag{2.3}$$

And for the TH-BPSK UWB system

$$s_{BPSK}^{(k)}(t,i)=\sqrt{\frac{E_b}{N_s}}\sum_{j=iN_s}^{(i+1)N_s-1}d_i^{(k)}p(t-jT_f-c_j^{(k)}T_c) \tag{2.4}$$

Where $s^{(k)}(t,i)$ is the transmitting signal for the i^{th} data bit, $p(t)$ is the signal pulse, normalized to have unit energy. The parameters used are in accordance with [9], [10], and [11].

- E_b is the bit energy
- T_f is the frame duration , and bit duration $T_b = N_s T_f$
- N_s is the number of frames used to transmit a bit of information
- N_h is the number of time hops
- T_c is the time hopped duration , where $N_h T_c \le T_f$
- $c_j^{(k)}$ is the k^{th} user's time hopping code. It is pseudorandom in nature which takes integer values in the range $0 \le c^{(k)} < N_h$.
- $d_i^{(k)}$ is the i^{th} data bit for the k^{th} user. For TH-BPSK $d_i^{(k)} \in \{1,-1\}$ and for TH-PPM $d_i^{(k)} \in \{0,1\}$
- δ is the modulation index for the PPM.

Suppose N_u users are actively operating, the received signal is

$$r(t) = \sum_{k=1}^{N_u} A_k s^{(k)}(t-\tau_k) + n(t) \tag{2.5}$$

Where $n(t)$ is the additive white noise with two-sided power spectral density $\frac{N_0}{2}$, A_k represent the channel amplitude impairment factor for the k^{th} user and τ_k is the time shift for N_u signals.

Assuming all users are transmitting asynchronously under perfect power control. At the receiver end, conventional correlation receiver is used to demodulate the desired signal. Further, assume that $s^{(1)}(t)$ is the desired signal and $d_0^{(1)}$ to be transmitted. For convenience, assume that $c_j^{(1)} = 0, \forall j$. The correlation receiver computes the decision variable as

$$r = \sqrt{\frac{N_s}{E_b}} \sum_{j=0}^{N_s-1} \int_{jT_f}^{(j+1)T_f} r(t) v(t-\tau_1 - jT_f) dt \tag{2.6}$$

Where $v(t)$ is a reference waveform.

$$r = S + I + n \tag{2.7}$$

Where S is the desired signal component, I is the interference from $N_u - 1$ users and n is the noise component.

The mean of the noise term is

$$\begin{aligned} \mathrm{E}[n] &= \mathrm{E}\left[\sqrt{\frac{N_s}{E_b}} \sum_{j=0}^{N_s-1} \int_{jT_f}^{(j+1)T_f} n(t) v(t-\tau_1 - jT_f) dt \right] \\ &= \sqrt{\frac{N_s}{E_b}} \sum_{j=0}^{N_s-1} \int_{jT_f}^{(j+1)T_f} \mathrm{E}[n(t)] v(t-\tau_1 - jT_f) dt \\ &= 0 \end{aligned} \tag{2.8}$$

And the variance is

$$\begin{aligned} \mathrm{var}[n] &= \mathrm{E}[n^2] \\ &= \frac{N_s}{E_b} \sum_{i=0}^{N_s-1} \sum_{j=0}^{N_s-1} \int_{iT_f}^{(i+1)T_f} \int_{jT_f}^{(j+1)T_f} \mathrm{E}[n(s)n(t)] \mathrm{E}[v(s-\tau_1 - iT_f) v(t-\tau_1 - jT_f)] dt ds \end{aligned}$$

$$= \frac{N_s}{E_b} \sum_{i=0}^{N_s-1} \sum_{j=0}^{N_s-1} \int_{iT_f}^{(i+1)T_f} \int_{jT_f}^{(j+1)T_f} \frac{N_0}{2} \delta(s-t) \mathrm{E}[v(s-\tau_1 - iT_f)v(t-\tau_1 - jT_f)]dtds$$

$$= \frac{N_s N_0}{2E_b} \sum_{j=0}^{N_s-1} \int_{jT_f}^{(j+1)T_f} \mathrm{E}[v^2(t)]dt \qquad (2.9)$$

If $T_f >> T_p$

$$= \frac{N_s^2 N_0}{2E_b} \int_{-\infty}^{\infty} v^2(t)dt \qquad (2.10)$$

2.3 Analysis of TH-PPM system

The performance analysis of the TH-PPM system based on the decision variable at the receiver end. In [5], [8], [9] and [11], systems consider information bits $d_i^{(k)} \in \{0,1\}$, and the reference waveform is

$$v(t) = p(t) - p(t-\delta) \qquad (2.11)$$

The autocorrelation of the Gaussian monocycle used, is given by

$$R(x) = \int_{-\infty}^{+\infty} p(t)p(t-x)dt \qquad (2.12)$$

$$R(x) = \left[1 - 4\pi\left(\frac{x}{\tau_p}\right)^2 + \frac{4\pi^2}{3}\left(\frac{x}{\tau_p}\right)^4\right] \exp\left[-\pi\left(\frac{x}{\tau_p}\right)^2\right] \qquad (2.13)$$

$$R(0) = 1 \qquad (2.14)$$

Correlation of the reference waveform $v(t)$ with the time-shifted pulse $p(t)$ is

$$\tilde{R}(x) = \int_{-\infty}^{\infty} p(t-x)v(t)dt$$

$$= \int_{-\infty}^{\infty} p(t-x)[p(t) - p(t-\delta)]dt$$

$$= R(x) - R(x-\delta) \qquad (2.15)$$

$$\tilde{R}(0) = R(0) - R(-\delta)$$

$$= 1 - R(-\delta) \qquad (2.16)$$

The variance of noise component is

$$\sigma_n^2 = \mathrm{E}[n^2] = \frac{N_s^2 N_0}{2E_b} \int_{-\infty}^{\infty} v^2(t)dt$$

$$= \frac{N_s^2 N_0}{2E_b} \int_{-\infty}^{\infty} \left[p^2(t) + p^2(t-\delta) - 2p(t)p(t-\delta) \right] dt$$

$$= \frac{N_s^2 N_0}{2E_b} \left[2R(0) - 2R(-\delta) \right]$$

$$= \frac{N_s^2 N_0}{E_b} \tilde{R}(0) \tag{2.17}$$

From equation (2.7)

$$S = \int_{-\infty}^{\infty} A_1 s^{(1)}(t-\tau_1) v(t)dt$$

$$= \sum_{j=iN_s}^{(i+1)N_s-1} A_1 \int_{jT_f}^{(j+1)T_f} p(t - jT_f - c_j^{(1)} T_c - d_i^{(1)}\delta) v(t - jT_f)dt$$

$$= \pm A_1 N_s \tilde{R}(0) \tag{2.18}$$

And I is the total multi-user interference due to $N_u - 1$ users

$$I = \int_{-\infty}^{\infty} \sum_{k=2}^{N_u} s^k(t-\tau_k) v(t)dt$$

$$= \sqrt{\frac{N_s}{E_b}} \sum_{k=2}^{N_u} \sum_{j=0}^{N_s-1} \int_{jT_f}^{(j+1)T_f} A_k s^{(k)}(t-\tau_k) v(t - jT_f - \tau_1)dt \tag{2.19}$$

The time difference asynchronous users is modeled as

$$\tau_k - \tau_1 = j_k T_f + \alpha_k \ , \qquad -\frac{T_f}{2} \le \alpha_k < \frac{T_f}{2} \tag{2.20}$$

Where j_k is the value of the time difference $\tau_k - \tau_1$ rounded to the nearest frame time.

Expression for I can be written as

$$I = \sum_{k=2}^{N_u} \sum_{j=0}^{N_s-1} \int_{-\infty}^{\infty} A_k p(x - \alpha_k - c_j^{(k)} T_c - d_{\lfloor (j+j_k)/N_s \rfloor}^{(k)} \delta) v(x)dx \tag{2.21}$$

Consider that $d_{\lfloor (j+j_k)/N_s \rfloor}^{(k)}$ may change sign during the transmission time of $d_0^{(1)}$,

$$I=\sum_{k=2}^{N_u}A_k\left[\sum_{j=0}^{\gamma_k-1}\int_{-\infty}^{\infty}p(t-\alpha_k-c_j^{(k)}T_c-d_{\lfloor (j+j_k)/N_s\rfloor}^{(k)}\delta)v(t-jT_f)dt+\sum_{\gamma_k}^{N_s-1}\int_{-\infty}^{\infty}p(t-\alpha_k-c_j^{(k)}T_c-d_{\lfloor (j+j_k)/N_s\rfloor}^{(k)}\delta)v(t\right.$$

$$=\sum_{k=2}^{N_u}A_k\left[\sum_{j=0}^{\gamma_k-1}\tilde{R}(\tilde{\theta}_{0,j})+\sum_{j=\gamma_k}^{N_s-1}\tilde{R}(\tilde{\theta}_{1,j})\right] \qquad (2.22)$$

Where

$$\tilde{\theta}_{0,j}^{(k)}=\alpha_k+c_j^{(k)}T_c+d_0^{(k)}\delta \qquad (2.23)$$

$$\tilde{\theta}_{1,j}^{(k)}=\alpha_k+c_j^{(k)}T_c+d_1^{(k)}\delta \qquad (2.24)$$

Where $d_0^{(k)}$ and $d_1^{(k)}$ are the adjacent interfering bits from the k^{th} user's transmitting system meanwhile the transmission of d_0^1, and $\gamma_k\in[0,N_s-1]$.The probability density function (PDF) of $\tilde{\theta}_{0,j}^{(k)}$, conditioned on $d_0^{(k)}$ for a given α_k becomes

$$f_{\tilde{\theta}_{0/d,\alpha}}(\tilde{\theta}/d_0^{(k)}=d,\alpha_k=\alpha)=\frac{1}{N_h}\sum_{h=0}^{N_h-1}\delta_D(\tilde{\theta}-hT_c-\delta d-\alpha) \qquad (2.25)$$

Where $\delta_D(.)$ is a Dirac delta function.

The characteristic function (CHF) conditioned on $d_0^{(k)}$ and α_k can be written as

$$\phi_{\tilde{R}_{0/d,\alpha}}(\omega)=\int_{-\infty}^{\infty}f_{\tilde{\theta}_{0/d,\alpha}}(\tilde{\theta}/d_0^{(k)}=d,\alpha_k=\alpha)e^{j\omega\tilde{R}(\tilde{\theta}_{0,j})}d\tilde{\theta}$$

$$=\frac{1}{N_h}\sum_{h=0}^{N_h-1}e^{j\omega\tilde{R}(\alpha+hT_c+\delta d)} \qquad (2.26)$$

Defining $X^{(k)}=\sum_{j=0}^{\gamma_k-1}\tilde{R}(\tilde{\theta}_{0,j})$ and $Y^{(k)}=\sum_{j=\gamma_k}^{N_{\theta s}-1}\tilde{R}(\tilde{\theta}_{1,j})$

$$I=\sum_{k=2}^{N_u}A_kI^{(k)}$$

$$=\sum_{k=2}^{N_u}A_k(X^{(k)}+Y^{(k)}) \qquad (2.27)$$

The conditional CHF of $X^{(k)}$ is given by

$$\varphi_{X^{(k)}/d,\alpha,\gamma}=\mathrm{E}[e^{j\omega X^{(k)}}/d_0^{(k)}=d,\alpha_k=\alpha,\gamma_k=\gamma]$$

$$= \mathrm{E}\left[e^{j\omega \sum_{j=0}^{\gamma_k - 1} \tilde{R}(\tilde{\theta}_{0,j})} / d_0^{(k)} = d, \alpha_k = \alpha, \gamma_k = \gamma \right]$$

$$= \prod_{j=0}^{\gamma_k - 1} \varphi_{\tilde{R}_{0/d,\alpha}}(\omega)$$

$$= \left\{ \frac{1}{N_h} \sum_{h=0}^{N_h - 1} e^{j\omega \tilde{R}(\alpha + hT_c + \delta d)} \right\}^{\gamma} \tag{2.28}$$

Where $\tilde{R}(\theta_{0,j}), j = 0,1,2,3.....\gamma_k - 1$ are independent conditioned on $d_0^{(k)}$ and α_k.

The CHF of $X^{(k)}$ conditioned on α_k and γ_k can be obtained using the theorem of total probability as

$$\varphi^{(k)}_{X^{(k)}/\alpha,\gamma}(\omega) = \varphi^{(k)}_{X^{(k)}/0,\alpha,\gamma}(\omega)\Pr(d=0) + \varphi^{(k)}_{X^{(k)}/1,\alpha,\gamma}(\omega)\Pr(d=1)$$

Assuming that bits are equiprobable with probabilities, $\Pr(d=0) = \Pr(d=1) = \frac{1}{2}$

$$= \frac{1}{2}\left\{ \frac{1}{N_h} \sum_{h=0}^{N_h - 1} e^{j\omega \tilde{R}(\alpha + hT_c)} \right\}^{\gamma} + \frac{1}{2}\left\{ \frac{1}{N_h} \sum_{h=0}^{N_h - 1} e^{j\omega \tilde{R}(\alpha + hT_c + \delta)} \right\}^{\gamma}$$

$$= \frac{1}{2N_h^{\gamma}}\left[\left\{ \sum_{h=0}^{N_h - 1} e^{j\omega \tilde{R}(\alpha + hT_c)} \right\}^{\gamma} + \left\{ \sum_{h=0}^{N_h - 1} e^{j\omega \tilde{R}(\alpha + hT_c + \delta)} \right\}^{\gamma} \right] \tag{2.29}$$

Similarly the CHF of $Y^{(k)}$, conditioned on α_k and γ_k can be obtained as

$$\varphi_{Y^{(k)}/\alpha,\gamma} = \frac{1}{2N_h^{(N_s - \gamma)}}\left[\left\{ \sum_{h=0}^{N_h - 1} e^{j\omega \tilde{R}(\alpha + hT_c)} \right\}^{N_s - \gamma} + \left\{ \sum_{h=0}^{N_h - 1} e^{j\omega \tilde{R}(\alpha + hT_c + \delta)} \right\}^{N_s - \gamma} \right] \tag{2.30}$$

Since random variables (RV's) $X^{(k)}$ and $Y^{(k)}$ are independent due to independence between d_0 and d_1. The CHF of $I^{(k)}$ conditioned on α_k and γ_k is given by

$$\varphi_{I^{(k)}/\alpha,\gamma}(\omega) = \varphi_{X^{(k)}/\alpha,\gamma}(\omega)\varphi_{Y^{(k)}/\alpha,\gamma}(\omega) \tag{2.31}$$

We considered γ_k uniformly distributed over $[0, N_s - 1]$. Then, we can rewrite CHF of $I^{(k)}$ conditioned on α_k as

$$\varphi_{I^{(k)}/\alpha}(\omega) = \frac{1}{N_s} \sum_{\gamma=0}^{N_s - 1} \varphi_{X^{(k)}/\alpha,\gamma}(\omega)\varphi_{Y^{(k)}/\alpha,\gamma}(\omega) \tag{2.32}$$

The CHF for the k^{th} user can be obtained by averaging out α_k

$$\varphi_{I^{(k)}}(\omega) = \frac{1}{T_f} \int_{\frac{-T_f}{2}}^{\frac{T_f}{2}} \varphi_{I^{(k)}/\alpha}(\omega) dt \tag{2.33}$$

All interfering components are independent to each other; the CHF of total interference is given as

$$\varphi_I(\omega) = \prod_{k=2}^{N_u} \varphi_{I^{(k)}}(A_k \omega) \tag{3.34}$$

2.4 Analysis of TH-BPSK system

The BER performance analysis of TH-BPSK system is in accordance with [10], [11]. In this, we consider the information bits $d_i^{(k)} \in \{-1, 1\}$ and the reference waveform is the pulse $p(t)$. The decision variable for TH-BPSK system is given by

$$r_{BPSK} = S_{BPSK} + I_{BPSK} + n_{BPSK} \tag{2.35}$$

Where n_{BPSK} is the Gaussian noise with zero mean and variance

$$\sigma_{BPSK}^2 = \frac{N_0 N_s^2}{2E_b} \int_{-\infty}^{\infty} v^2(t) dt$$

$$= \frac{N_0 N_s^2}{2E_b} \int_{-\infty}^{\infty} p^2(t) dt$$

$$= \frac{N_0 N_s^2}{2E_b} R(0) = \frac{N_0 N_s^2}{2E_b} \tag{2.36}$$

And $$S_{BPSK} = \int_{-\infty}^{\infty} A_1 s^1(t - \tau_1) v(t) dt$$

$$= \sum_{j=iN_s}^{(i+1)N_s - 1} A_1 \int_{jT_f}^{(j+1)T_f} d_0^{(1)} p(t - jT_f - c_j^{(1)} T_c) p(t - jT_f - c_j^{(1)} T) dt$$

$$= d_0^{(1)} A_1 N_s R(0)$$

$$= d_0^{(1)} A_1 N_s \tag{2.37}$$

I_{BPSK} is the total multi-user interference and is given by

$$I_{BPSK}^{(k)} = \int_{-\infty}^{\infty} \sum_{k=2}^{N_u} s^{(k)}(t-\tau_k) v(t) dt$$

$$= \sum_{k=2}^{N_u} \sum_{j=0}^{N_s-1} d_{\lfloor j/N_s \rfloor}^{(k)} \int_{jT_f}^{(j+1)T_f} p(t-jT_f - c_j^{(k)} T_c - \tau_k) p(t-jT_f) dt$$

$$= \sum_{k=2}^{N_u} \sum_{j=0}^{N_s-1} d_{\lfloor j/N_s \rfloor}^{(k)} \int_{jT_f}^{(j+1)T_f} p(t-j_k T_f - c_j^{(k)} T_c - \alpha_k) p(t-jT_f) dt$$

$$= \sum_{k=2}^{N_u} A_k \left[\sum_{j=0}^{\gamma_k-1} d_0^{(k)} \int_{jT_f}^{(j+1)T_f} p(t-j_k T_f - c_j^{(k)} T_c - \alpha_k) p(t-jT_f) dt + \sum_{j=\gamma_k}^{N_s-1} d_1^{(k)} \int_{jT_f}^{(j+1)T_f} p(t-j_k T_f - c_j^{(k)} T_c - \alpha_k) p(t \right.$$

$$= \sum_{k=2}^{N_u} A_k \left[\sum_{j=0}^{\gamma_k-1} d_0^{(k)} R(\theta_j^{(k)}) + \sum_{j=\gamma_k}^{N_s-1} d_1^{(k)} R(\theta_j^{(k)}) \right] \quad (2.38)$$

Where $\theta_j^{(k)} = \alpha_k + c_j^{(k)} T_c$

The PDF of $\theta_j^{(k)}$ conditioned on $d_0^{(k)}$ for a given α_k becomes

$$f_{\theta/\alpha}(\theta / \alpha_k = \alpha) = \frac{1}{N_h} \sum_{h=0}^{N_h-1} \delta_D(\theta - hT_c - \alpha) \quad (2.39)$$

Then the CHF of $R(\theta_j^{(k)})$ conditioned on α_k can be obtained as

$$\varphi_{R/\alpha}(\omega) = \mathrm{E}[e^{j\omega R(\theta_j^{(k)})} / \alpha_k = \alpha]$$

$$= \int_{-\infty}^{\infty} f_{\theta/\alpha}(\theta / \alpha_k = \alpha) e^{j\omega R(\theta_j^{(k)})} d\theta$$

$$= \frac{1}{N_h} \int_{-\infty}^{\infty} \sum_{h=0}^{N_h-1} \delta_D(\theta - hT_c - \alpha) e^{j\omega R(\theta_j^{(k)})} d\theta$$

$$= \frac{1}{N_h} \sum_{h=0}^{N_h-1} e^{j\omega R(\alpha + hT_c)} \quad (2.40)$$

Again defining

$$I_{BPSK} = \sum_{k=2}^{N_u} A_k I_{BPSK}^{(k)}$$

$$= \sum_{k=2}^{N_u} A_k \left[X_{BPSK}^{(k)} + Y_{BPSK}^{(k)} \right] \quad (2.41)$$

Where $X_{BPSK}^{(k)} = \sum_{j=0}^{\gamma_k - 1} d_0^{(k)} R(\theta_j^{(k)})$ and $Y_{BPSK}^{(k)} = \sum_{j=\gamma_k}^{N_s - 1} d_1^{(k)} R(\theta_j^{(k)})$

The CHF of $X_{BPSK}^{(k)}$ conditioned on α_k and γ_k is obtained as

$$\varphi_{X^{(k)}/\alpha,\gamma} = E[e^{j\omega X^{(k)}} / d_0^{(k)} = d, \alpha_k = \alpha, \gamma_k = \gamma]$$

$$= \left[\frac{1}{N_h} \sum_{h=0}^{N_h - 1} e^{j\omega d_0^{(k)} R(\theta_j^{(k)})} \right]^{\gamma} \tag{2.42}$$

$$\varphi_{X^{(k)}/\alpha,\gamma}^{(k)}(\omega) = \varphi_{X^{(k)}/-1,\alpha,\gamma}^{(k)}(\omega) \Pr(d = -1) + \varphi_{X^{(k)}/1,\alpha,\gamma}^{(k)}(\omega) \Pr(d = 1)$$

$$= \frac{1}{2} \left\{ \frac{1}{N_h} \sum_{h=0}^{N_h - 1} e^{j\omega R(\theta_j^{(k)})} \right\}^{\gamma} + \frac{1}{2} \left\{ \frac{1}{N_h} \sum_{h=0}^{N_h - 1} e^{-j\omega R(\theta_j^{(k)})} \right\}^{\gamma}$$

$$= \frac{1}{2N_h^{\gamma}} \left[\left\{ \sum_{h=0}^{N_h - 1} e^{j\omega R(\alpha + hT_c)} \right\}^{\gamma} + \left\{ \sum_{h=0}^{N_h - 1} e^{-j\omega R(\alpha + hT_c)} \right\}^{\gamma} \right] \tag{2.43}$$

Similarly the conditional CHF of $Y_{BPSK}^{(k)}$ is given by

$$\varphi_{Y^{(k)}/\alpha,\gamma} = \frac{1}{2N_h^{N_s - \gamma}} \left[\left\{ \sum_{h=0}^{N_h - 1} e^{j\omega R(\alpha + hT_c)} \right\}^{N_s - \gamma} + \left\{ \sum_{h=0}^{N_h - 1} e^{-j\omega R(\alpha + hT_c)} \right\}^{N_s - \gamma} \right] \tag{2.44}$$

The CHF of $I_{BPSK}^{(k)}$ conditioned on α_k and γ_k is given by

$$\varphi_{I_{BPSK}^{(k)}/\alpha,\gamma}(\omega) = \varphi_{X_{BPSK}^{(k)}/\alpha,\gamma}(\omega) \varphi_{Y_{BPSK}^{(k)}/\alpha,\gamma}(\omega) \tag{2.45}$$

Consider that $\{\alpha_k\}_{k=2}^{N_u}$ and $\{\gamma_k\}_{k=2}^{N_u}$ are uniformly distributed, then CHF of $I_{BPSK}^{(k)}$ can be rewritten as

$$\varphi_{BPSK}^{(k)} = \frac{1}{N_s T_f} \int_{-\frac{T_f}{2}}^{\frac{T_f}{2}} \sum_{\gamma=0}^{N_s - 1} \varphi_{X_{BPSK}^{(k)}/\alpha,\gamma}(\omega) \varphi_{Y_{BPSK}^{(k)}/\alpha,\gamma}(\omega) d\alpha \tag{2.46}$$

The CHF of total interference is given by

$$\varphi_{BPSK} = \prod_{k=2}^{N_u} \phi_{I_{BPSK}^{(k)}}(A_k \omega) \tag{2.47}$$

2.5 Bit Error Probability Calculation

2.5.1 Bit Error Probability Calculation for TH-PPM

The decision variable for the TH-PPM system according to [5], [10] and [11] is

$$r > 0 \Rightarrow \text{"0"}$$

$$r \leq 0 \Rightarrow \text{"1"}$$

The average probability of error for TH-PPM system, considering the symmetry of the MAI and the noise is given by

$$P_e = \Pr(r \leq 0 / d = 0)$$

$$= \Pr(A_1 N_s \bar{R}(0) + I + n \leq 0) \tag{2.48}$$

Define, $\Lambda = I + n$

The characteristic function of Λ can be expressed as

$$\varphi_\Lambda(\omega) = \varphi_I(\omega)\varphi_n(\omega) \tag{2.49}$$

It's from the assumption that MAI and additive white noise is independent where

$$\varphi_n(\omega) = e^{-\frac{\sigma_n^2 \omega^2}{2}} \tag{2.50}$$

The cumulative density function (CDF) of Λ can be obtained by taking inverse transform of the characteristic function, and is given by

$$F_\Lambda(\lambda) = \frac{1}{2} + \frac{1}{\pi}\int_0^\infty \frac{Sin(\lambda\omega)}{\omega}\varphi_\Lambda(\omega)d\omega \tag{2.51}$$

The bit error rate (BER) is given by

$$P_e = \Pr(A_1 N_s \bar{R}(0) + I + n \leq 0)$$

$$= 1 - F_\Lambda(A_1 N_s \bar{R}(0)) \tag{2.52}$$

Substituting the value of CDF from equations (2.49) and (2.51)

$$P_e = 1 - \frac{1}{\pi}\int_0^\infty \frac{Sin(A_1 N_s \bar{R}(0)\omega)}{\omega}\varphi_I(\omega)e^{-\frac{\sigma_n^2\omega^2}{2}}d\omega \tag{2.53}$$

2.5.2 Bit Error Probability Calculation for TH-BPSK

Decision variable for TH-BPSK according to [9], [10] and [11] is given by

$$r > 0 \Rightarrow \text{"1"}$$

$$r < 0 \Rightarrow \text{"}-1\text{"}$$

The average probability of error for TH-BPSK system, considering the symmetry of the MAI and the noise is given by

$$\begin{aligned} P_e &= \Pr(r \le 0 / d = 1) \\ &= \Pr(A_1 N_s + I + n \le 0) \end{aligned}$$

Where $R(0) = 0, d_0^{(1)} = d = 1$

$$= 1 - F_\Lambda(AN_s)$$

$$= 1 - \frac{1}{\pi} \int_0^\infty \frac{Sin(A_1 N_s \omega)}{\omega} \varphi_{I_{BPSK}}(\omega) e^{\frac{-\sigma_{nBPSK}^2 \omega^2}{2}} d\omega \qquad (2.54)$$

2.6 Simulation results and comparisons

In this section, we present some performance results for analysis in sections 2.3 and 2.4. We simulated the decision variables indicated in equations (2.7) and (2.35). The parameters used for the simulation and their typical values are listed in table I. In our simulation, we restrict our calculation of the BER for TH-PPM and TH-BPSK systems to the second-order Gaussian monocycle. However, simulation can be run for arbitrary pulse shapes with different values of N_s.

TABLE-I

VALUE OF THE PRINCIPAL PARAMETERS FOR THE ANALYZED SYSTEM

Parameter	Symbol	Typical Value
Time Normalizing factor	τ_p	0.05 ns
Impulse Width	T_p	0.9 ns
Frame Width	T_f	7.2 ns
Modulation Index	δ	0.15 ns
Chip Width	T_c	0.9 ns
Number of users	N_u	8, 16
Number of Hopes	N_h	8, 16
Repetition Code Length	N_s	2, 4

First, we compare the BER of the TH-PPM and TH-BPSK systems with results obtained from simulations. In fig.2.2, the BER curves of the TH-PPM and TH-BPSK systems are presented as a function of $\frac{E_b}{N_o}$ with $N_s = 2$. The solid lines marked by circles and triangles are BER curves for TH-BPSK and TH-PPM respectively. From fig. 2.2, it is cleared that BPSK outperforms than PPM for all values of SNR, but for medium and large values of SNR this difference in BER is greater than the small values of SNR.

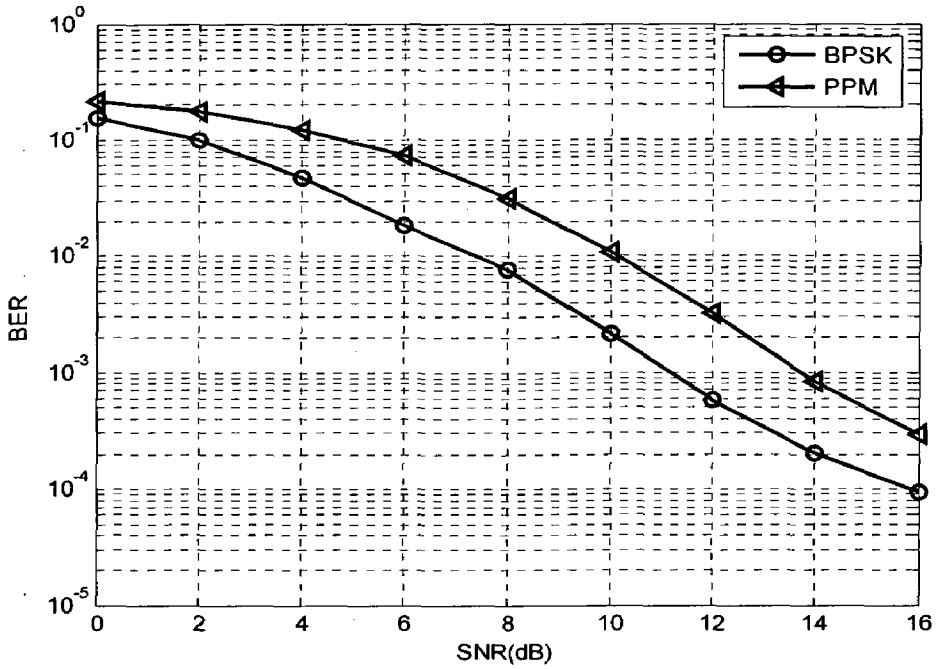

Fig. 2.2 Comparison of the TH-BPSK and TH-PPM systems for a repetition code N_s=2 assuming 7 asynchronous interferers.

The BER performance of the TH-PPM UWB system for different Gaussian monocycles and different pulse widths is examined in fig.2.3 and fig.2.4. We can see in fig.2.3, that the system using doubly differentiated Gaussian monocycle as transmitting pulse outperforms the system using Gaussian pulse. BER performance of the TH-PPM system is evaluated in [10] for 2^{nd} order and 4^{th} order Gaussian monocycles. From the simulation results shown in fig.2.3 and in [10], it is cleared that on increasing the pulse order, system performs better in terms of BER.

Fig.2.4 shows the BER performance of the TH-PPM system for time normalizing factor $\tau_p = 0.05\,\text{ns}$ and $\tau_p = 0.2\,\text{ns}$. From equation (2.16) and (2.17), it can be inferred that, smaller values of $\tilde{R}(0)$ will lead to degradation of the system performance. Results obtained from simulation indicates that pulse timing factor $\tau_p = 0.2\,\text{ns}$ gives better results than $\tau_p = 0.05\,\text{ns}$ which supports the interpretation of equation (2.16). For this simulation, we have taken $N_h = 16$, $N_u = 16$ and $N_s = 2$.

Equations (2.3) and (2.4) indicate that an information bit is represented by N_s pulses. If we increase the number of pulses per bit, $\frac{E_b}{N_o}$ increases, consequently system performance would improve. Our simulation performed for both TH-PPM and TH-BPSK systems for $N_s = 2$ and $N_s = 4$ shows that system using $N_s = 4$ pulses performs better than the system using $N_s = 2$ pulses for an information bit. Fig.2.5 and fig.2.6 shows the BER curves for TH-PPM and TH-BPSK systems which support the argument.

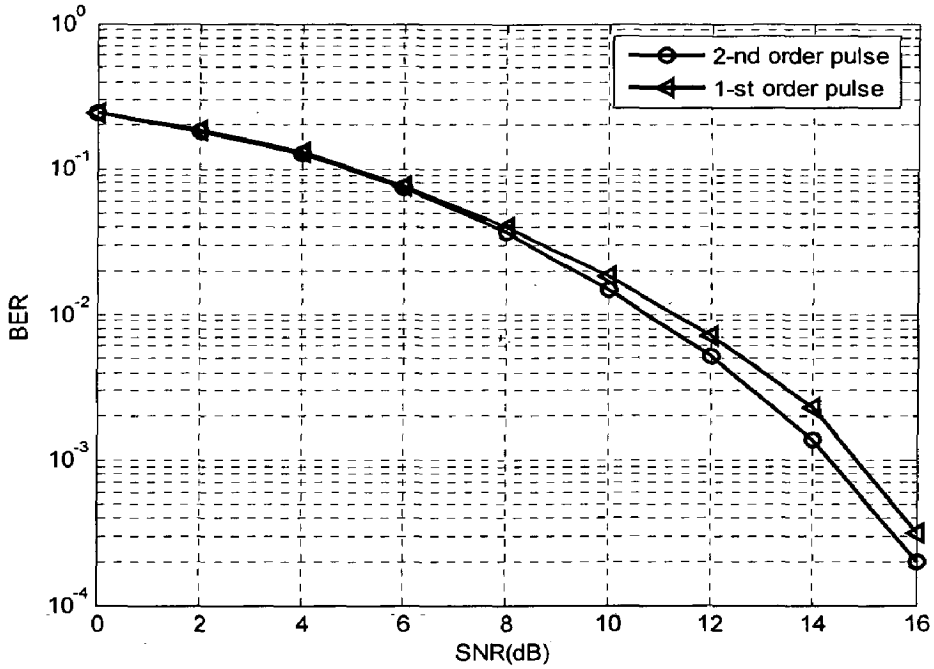

Fig.2.3 Comparison of the TH-PPM systems using different Gaussian monocycles for a repetition code with N_s=2 assuming 7 asynchronous interferers .

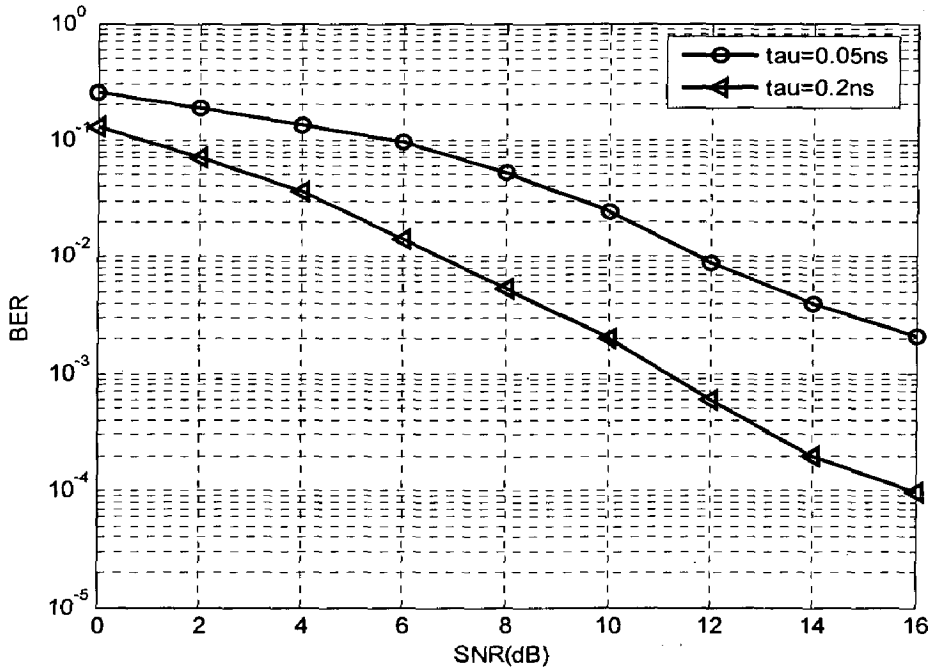

Fig.2.4 BER of the TH-PPM system versus SNR for $\tau_p = 0.05$ ns and $\tau_p = 0.2$ ns assuming 15 asynchronous interferers with N_h=16.

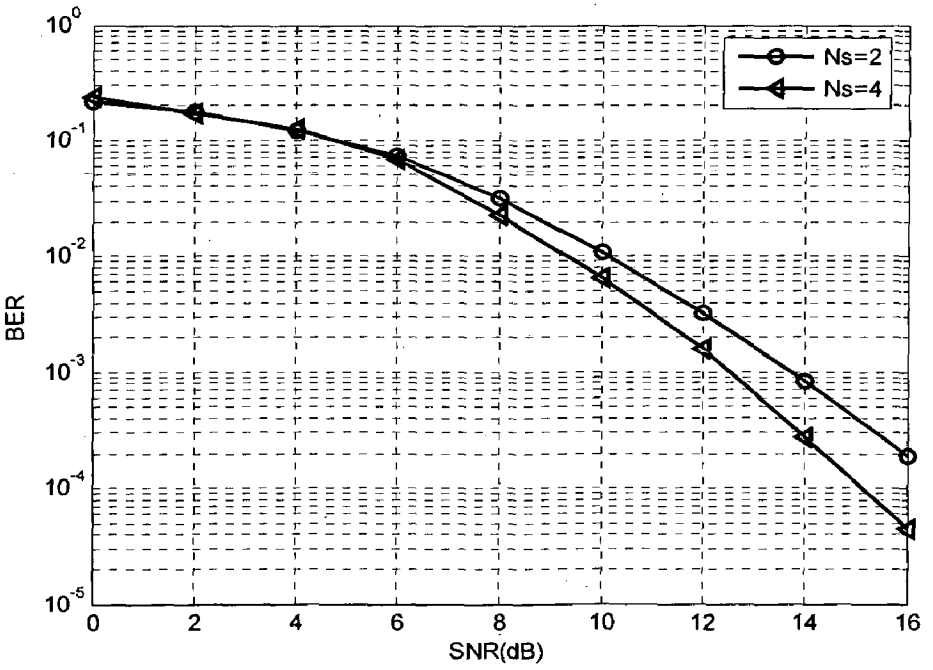

Fig.2.5 BER of the TH-PPM UWB system versus SNR for repetition code with N_s=2 and N_s=4 assuming 7 asynchronous interferers.

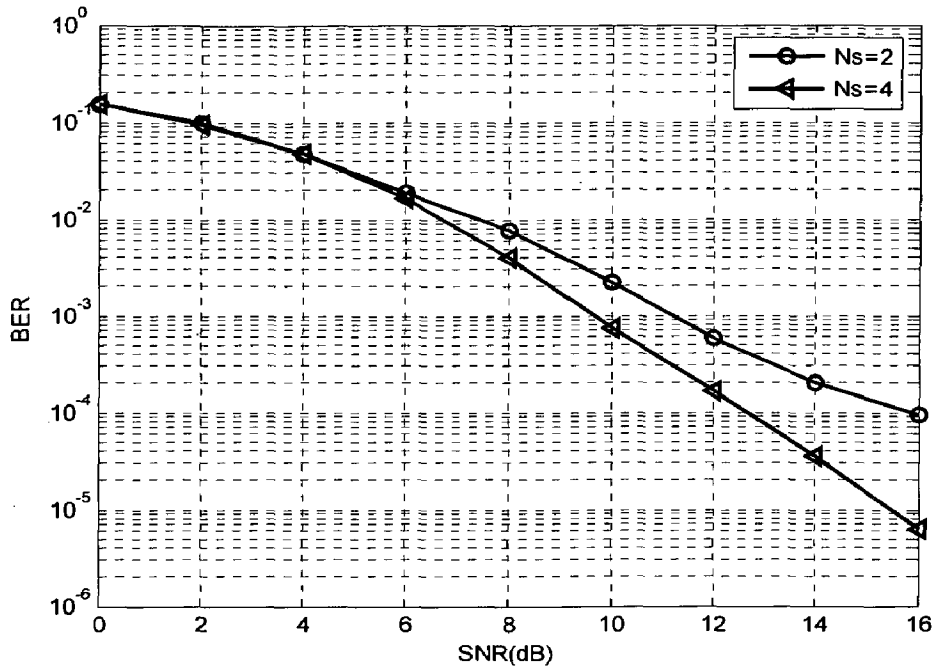

Fig. 2.6 BER of the TH-BPSK UWB system versus SNR for a repetition code N_s=2 and N_s=4 assuming 7 asynchronous interferers

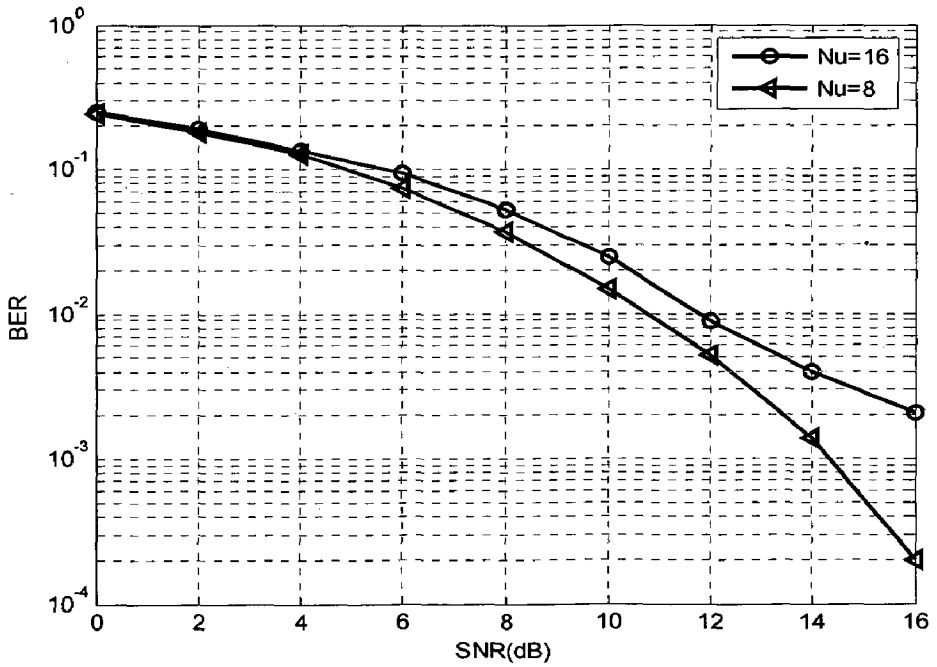

Fig.2.7 Comparison of the TH-PPM systems with 7 and 15 asynchronous interferers for N_h=16 and N_s=2.

In multiple access scenarios, signals transmitted by users other than the desired user add up and gives rise to multiple access interference (MAI). The MAI increases as the active number of users increases in the network. Simulation results obtained for 7 and 15 asynchronous interferers show that large number of active users worsens the performance of the UWB system. Fig.2.7 proves that BER is more for 15 active users than the 7 users.

Chapter 3

Performance Evaluation of Multiple Access in DS-PPM and DS-BPSK UWB-IR Systems

3.1 Introduction

Ultra-wideband (UWB) technology has gained tremendous attention from both industry and academia. Both researchers and standardization communities are interested in it, due to, its promising ability to provide high data rate at low cost and complexity. The very small value of power spectral density of the UWB signal ensures the undetectability of the signal by unintended users which looks noise like signal to others. The ultra-wide bandwidth makes the UWB systems suitable for multiple access applications.

Time hopping combined with pulse position modulation has been the original proposal for UWB communication systems. It eliminates catastrophic collisions in multiple accessing. UWB systems are classified as single band and multi band transmission systems. Single band systems consist time hopping spread spectrum (TH-SS) and direct sequence spread spectrum (DS-SS). TH-SS systems have been studied in [5], [8], [10] and [12]. In this chapter, we will analyze the DS-SS systems for pulse position and phase shift keying modulation schemes.

Direct sequence spread spectrum (DS-SS) is a well known and powerful multiple access technology. DS-UWB systems have been investigated in [17], [18], [22] and [25]. Coded DS-PPM system is analyzed in [24]. In DS-UWB, multiple pulses per bit period are transmitted based upon a certain spreading code. This method is robust against multi user interference and has low peak-to-average power ratio. Issues related with processing gain, jamming margin and coding gain for DS-UWB have been discussed in [20].

In this chapter, we discussed and obtained the simulation results for DS-UWB systems for pulse position modulation and binary phase shift keying modulation. The organization of this chapter is as follows. In section 3.2, we have shown system models. Section 3.3 and 3.4 are devoted in analysis of DS-PPM and DS-BPSK systems. BER

calculation, discussion on simulation results and comparisons are presented in sections 3.5 and 3.6 respectively.

3.2 System Model

In this section, we consider a direct sequence spread spectrum (DS-SS) UWB system with N_u users actively operating asynchronously. In a typical DS-SS scheme, a DS-BPSK UWB signal is written as

$$s_{DS-BPSK}^{(k)}(t) = \sqrt{\frac{E_b}{N_c}} \sum_{j=-\infty}^{\infty} \sum_{n=0}^{N_c-1} d_j^{(k)} c_n^{(k)} p(t - jT_f - nT_c) \tag{3.1}$$

And a DS-PPM UWB system is given as

$$s_{DS-PPM}^{(k)}(t) = \sqrt{\frac{E_b}{N_c}} \sum_{j=-\infty}^{\infty} \sum_{n=0}^{N_c-1} c_n^{(k)} p(t - jT_f - nT_c - \delta d_j^{(k)}) \tag{3.2}$$

All the system parameters are in accordance with [11]. Where $p(t)$ represents the transmitted waveform, $\{d_j^{(k)}\}$ the information bit for the k^{th} user, and $\{c_n^{(k)}\}$ are the spreading chips. The pseudo-random codes are used to distinguish the users and smooth spectrum. PN codes take values $\{-1, 1\}$. The length of the PN code affects the performance of the system. E_b and N_c represent bit energy and number of pulses respectively. T_c is chip duration. The processing gain for DS-UWB defined in [20] is $\frac{T_b}{T_c} = \frac{N_c T_c}{T_c} = N_c$. As we increase the processing gain, throughput reduces, because it takes more pulses to transmit an information bit. However, the BER performance improves by increasing processing gain.

Suppose N_u users are actively operating, the composed received signal $r(t)$ is given by

$$r(t) = \sum_{k=1}^{N_u} A_k s^{(k)}(t - \tau_k) + n(t) \tag{3.3}$$

In which A_k represents the attenuation factor for the k^{th} user. The random variable τ_k is the time delay caused by asynchronous transmission, and $n(t)$ represents the noise present at the receiver input modeled as $N(0,\sigma_{DS}^2)$.

3.3 Analysis of DS-BPSK System

The decision statistics for the correlator as given in [18] is

$$r_{DS} = \sum_{m=0}^{N_c-1} \int_0^{T_f} r(t) c_m^{(1)} p(t - mT_c) dt \tag{3.4}$$

It can be rewritten as

$$r_{DS} = S_{DS} + I_{DS} + n_{DS} \tag{3.5}$$

Where

$$\begin{aligned} S_{DS} &= \sum_{m=0}^{N_c-1} \int_0^{T_f} A_1 s^{(1)}(t-\tau_1) c_m^{(1)} p(t - mT_c) dt \\ &= \sum_{m=0}^{N_c-1} \sqrt{\frac{E_b}{N_c}} \int_0^{T_f} A_1 d_0^{(1)} c_m^{(1)} p(t - mT_c) c_m^{(1)} p(t - mT_c) dt \\ &= \sqrt{\frac{E_b}{N_c}} A_1 d_0^{(1)} \sum_{m=0}^{N_c-1} R(0) \\ &= \sqrt{E_b N_c} A_1 d_0^{(1)} \end{aligned} \tag{3.6}$$

And n_{DS} is a random variable with zero mean and variance $\sigma_{nDS}^2 = \frac{N_0 N_c}{2}$.

Finally, the total multi access interference I_{DS} is given by

$$I_{DS} = \sqrt{\frac{E_b}{N_c}} \sum_{k=2}^{N_u} A_k \sum_{m=0}^{N_c-1} \int_0^{T_f} s^{(k)}(t-\tau_k) c_m^{(1)} p(t - mT_c) dt \tag{3.7}$$

Where the spreading signal $c^{(k)}(t)$ for the k^{th} user is defined as

$$c^{(k)}(t) = \sum_{m=-\infty}^{\infty} c_m^{(k)} p(t - mT_c) \tag{3.8}$$

Defining the partial cross-correlation function between $c^{(k)}(t)$ and $c^{(1)}(t)$ as

$$R_{k,1}(\tau) = \int_0^{\tau} c^{(k)}(t-\tau)c^{(1)}(t)dt \tag{3.9}$$

And $$\hat{R}_{k,1}(\tau) = \int_{\tau}^{T_f} c^{(k)}(t-\tau)c^{(1)}(t)dt \tag{3.10}$$

The MUI can be written as

$$I_{DS} = \sqrt{\frac{E_b}{N_c}} \sum_{k=2}^{N_u} A_k \left[d_{-1}^{(k)} R_{k,1}(\tau_k) + d_0^{(k)} \hat{R}_{k,1}(\tau_k) \right]$$

$$= \sqrt{\frac{E_b}{N_c}} \sum_{k=2}^{N_u} A_k W_k \tag{3.11}$$

Where $W_k = d_{-1}^{(k)} R_{k,1}(\tau_k) + d_0^{(k)} \hat{R}_{k,1}(\tau_k)$. Defining the partial autocorrelation function of the pulse waveform as

$$R_p(s) = \int_0^{s} p(t)p(t+T_c-s)dt, \qquad 0 \le s \le T_c \tag{3.12}$$

$$\hat{R}_p(s) = \int_s^{T_c} p(t)p(t_c-s)dt, \qquad 0 \le s \le T_c \tag{3.13}$$

Also, modeling the time shift τ_k as $\tau_k = \gamma_k T_c + \alpha_k$. Where $\gamma_k = \left\lfloor \frac{\tau_k}{T_c} \right\rfloor$ and α_k is a uniformly distributed random variable over $[0, T_c)$. And, defining auxiliary random variable $Z_j^{(k)}, j = 0,1,2,.....N_c$ as

$$\begin{aligned} Z_j^{(k)} &= d_{-1}^{(k)} c_{j-\gamma_k+N_c}^{(k)} c_j^{(1)}, & j &= 0,1,.....\gamma_k - 1 \\ &= d_0^{(k)} c_{j-\gamma_k}^{(k)} c_j^{(1)}, & j &= \gamma_k .....N_c - 2 \\ &= d_0^{(k)} c_{N_c-\gamma_k-1}^{(k)} c_{N_c-1}^{(1)}, & j &= N_c - 1 \\ &= d_{-1}^{(k)} c_{N_c-\gamma_k-1}^{(k)} c_0^{(1)}, & j &= N_c \end{aligned} \tag{3.14}$$

Then, W_k can be simplified as

$$W_k = \Gamma_k \hat{R}_p(\alpha_k) + \Delta_k R_p(\alpha_k) \tag{3.15}$$

Where $\Gamma_k = \sum_{j=0}^{N_c-1} Z_j^{(k)}$, and $\Delta_k = \sum_{j=0}^{N_c-2} Z_j^{(k)} c_j^{(1)} c_{j+1}^{(1)} + Z_{N_c}^{(k)}$

Γ_k and Δ_k are sums of N_c independently and identically distributed (i.i.d) symmetric Bernoulli RVs, and are independent to each other. The probability density function (PDF) of Γ_k and Δ_k can be obtained as

$$p_{\Gamma_k}(j) = p_{\Delta_k}(j) = \binom{N_c}{\frac{j+N_c}{2}} 2^{-N_c}, \quad j = -N_c, 2-N_c, \ldots\ldots\ldots N_c-2, N_c \tag{3.16}$$

The characteristic function (CF) of W_k conditioned on α_k is given by

$$\varphi_{W_k/\alpha}(\omega) = \mathrm{E}[e^{j\omega W_k} / \alpha_k = \alpha]$$

$$= \left\{\cos[\omega \hat{R}_p(\alpha)].\cos[\omega R_p(\alpha)]\right\}^{N_c} \tag{3.17}$$

Assuming α_k as a uniformly distributed RV. The CHF of W_k can be rewritten as

$$\varphi_{W_k}(\omega) = \frac{1}{T_c}\int_0^{T_c}\left\{\cos[\omega \hat{R}_p(\alpha)].\cos[\omega R_p(\alpha)]\right\}^{N_c} d\alpha \tag{3.18}$$

The CHF of the total interference is given by

$$\varphi_{I_{DS}}(\omega) = \prod_{k=2}^{N_u} \varphi_{W_k}\left(A_k\sqrt{\frac{E_b}{N_c}}\omega\right) \tag{3.19}$$

3.4 Analysis of DS-PPM System

Decision variable is based on [21]. All the system parameters are in accordance with [11]. Considering the first user and $j = 0, \tau_1 = 0$. Further, assume that system is operating in perfect synchronization for the desired user; the correlation receiver computes the decision variable as

$$r_{DS-PPM} = \int_0^{T_f} r(t) \sum_{n=0}^{N_c-1} c_n^{(1)} v(t - nT_c) dt$$

Where $v(t)$ is a reference waveform and is given by $v(t) = p(t) - p(t-\delta)$.

$$= S_{DS-PPM} + I_{DS-PPM} + n_{DS-PPM} \tag{3.20}$$

Where, $S_{DS-PPM} = \int_0^{T_f} s^{(1)}(t) \sum_{n=0}^{N_c-1} c_n^{(1)} v(t-nT_c)dt$

$$= \sum_{n=0}^{N_c-1} \sqrt{\frac{E_b}{N_c}} \int_0^{T_f} A_1 p(t-nT_c-d_0^{(1)}\delta) v(t-nT_c)dt$$

$$= \pm A_1 \sqrt{E_b N_c}\, \bar{R}(0) \qquad (3.21)$$

And, the total interference from $K-1$ users I is given as

$$I = \int_0^{T_f} \sum_{k=2}^{N_u} A_k s^{(k)}(t-\tau_k) \sum_{n=0}^{N_c-1} c_n^{(1)} v(t-nT_c)dt$$

$$= \sum_{k=2}^{N_u} A_k \sqrt{\frac{E_b}{N_c}} \sum_{n=0}^{N_c-1} c_n^{(k)} p(t-nT_c-\tau_k-d_0^{(k)}\delta) \sum_{m=0}^{N_c-1} c_m^{(1)} v(t-mT_c)dt$$

$$= \sum_{k=2}^{N_u} A_k \sqrt{\frac{E_b}{N_c}} \sum_{n=0}^{N_c-1} c_n^{(k)} p(t-nT_c-\tau_k-d_0^{(k)}\delta) \sum_{m=0}^{N_c-1} c_m^{(1)} v(t-mT_c)dt$$

$$= \sum_{k=2}^{N_u} I_k \qquad (3.22)$$

There are probably two continuous bits from the k^{th} user overlapping with $d_0^{(1)}$. Now, modeling I_k as

$$I_k = \int_0^{T_f} s^{(k)}(t-\tau_k) \sum_{n=0}^{N_c-1} c_n^{(1)} v(t-nT_c)dt$$

$$= \int_0^{\tau_k} \sqrt{\frac{E_b}{N_c}} \sum_{m=0}^{N_c-1} c_m^{(k)} p(t-mT_c+T_c-\tau_k-d_{-1}^{(k)}\delta) \sum_{n=0}^{N_c-1} c_n^{(1)} v(t-nT_c)$$

$$+ \int_{\tau_k}^{T_f} \sqrt{\frac{E_b}{N_c}} \sum_{m=0}^{N_c-1} c_m^{(k)} p(t-mT_c-\tau_k-d_0^{(k)}\delta) \sum_{n=0}^{N_c-1} c_n^{(1)} v(t-nT_c) \qquad (3.23)$$

Where τ_k is uniformly distributed over $[0, T_c)$ and defined as $\tau_k = \gamma_k T_c + \Delta T$. Where $\gamma_k \in \{0,1,2,\ldots\ldots,N_c-1\}$ and $\Delta T \in [0, T_c)$.

Defining the partial correlation function $R(x)$ as

$$R(x) = \int_0^{T_c} v(t)p(t-x)dt, \qquad x \in [0, 2T_p)$$

$$= \int_0^{T_c} v(t)p(t-x+T_c)dt, \qquad x \in \left[3T_p, 5T_p\right)$$

$$= 0, \qquad \text{elsewhere} \tag{3.24}$$

If $x = \Delta T + d_i^{(k)}\delta$, then $R(\Delta T)$ and $R(\Delta T + \tau)$ become part of $R(x)$.

Defining A and C as independent random variables from the random property of $c_n^{(k)}$

$A = \sum_{n=0}^{\gamma_k - 1} c_n^{(1)} c_{n+N_c-\gamma_k}^{(k)}$ and $C = \sum_{n=\gamma_k}^{N_c-1} c_n^{(1)} c_{n-\gamma_k}^{(k)}$. Where A and C are Binomial random variables with conditional distributions as

$$f_{A/\gamma_k}(a) = \binom{\gamma_k}{\frac{a+\gamma_k}{2}} 2^{-\gamma_k}, \qquad a \in \{-\gamma_k, -\gamma_k + 2, \ldots\ldots \gamma_k - 2, \gamma_k\} \tag{3.25}$$

and

$$f_{C/\gamma_k}(a) = \binom{N_c - \gamma_k}{\frac{c+N_c-\gamma_k}{2}} 2^{-(N_c-\gamma_k)}, \tag{3.26}$$

Where $c \in \{-(N_c - \gamma_k), -(N_c - \gamma_k) + 2, \ldots\ldots N_c - \gamma_k - 2, N_c - \gamma_k\}$

Also defining random variables B and D, because of the random property of $d_i^{(k)}$ as

$B = R(\Delta T + d_{-1}^{(k)}\delta)$ and $D = R(\Delta T + d_0^{(k)}\delta)$.

The B and D are i.i.d symmetric RVs as their conditional distributional is given by

$$P_{B/\Delta T}(x) = P_{D/\Delta T}(x) = 0.5, \qquad x = R(\Delta T)$$

$$= 0.5, \qquad x = R(\Delta T + T_p) \tag{3.27}$$

For the given values of ΔT and γ_k, the four random variables A, B, C and D are statistically independent. And based on ΔT and γ_k, the conditional distribution for I_k is given as

$$I_k = \sqrt{\frac{E_b}{N_c}}\left[A.B + C.D\right] \tag{3.28}$$

$$f_{I_k/\Delta T,\gamma_k}(x)=\frac{1}{2^{N_c+2}}\sum_{n=0}^{\gamma_k}\binom{\gamma_k}{n}\left[\delta[x-(2n-\gamma_k)R(\Delta T+\tau)]+\delta[x-(2n-\gamma_k)R(\Delta T)]\right]$$
$$\otimes\sum_{n=0}^{N_c-\gamma_k}\binom{N_c-\gamma_k}{n}\left[\delta[x-(2n-N_c+\gamma_k).R(\Delta T+\delta)]+\delta[x-(2n-N_c+\gamma_k).R(\Delta T)]\right] \quad (3.29)$$

Where $\otimes$ is a convolution symbol. The unconditional pdf of I_k is obtained by averaging ΔT and γ_k.

$$f_{I_k}(x)=\int_0^{T_c}\frac{1}{N_cT_c}\sum_{\gamma_k=0}^{N_c-1}f_{I_k/\Delta T,\gamma_k}(x)d\Delta T \quad (3.30)$$

And the characteristic function of I_k is given as

$$\varphi_{I_k}(\omega)=\int_{-\infty}^{\infty}f_{I_k}(x)e^{j\omega x}dx \quad (3.31)$$

From the assumption that all the N_u-1 interfering users are mutually independent. Therefore, the characteristic function of the total interference I is given as

$$\varphi_I=\prod_{k=2}^{N_u}\varphi_{I_k} \quad (3.32)$$

3.5 Bit Error Probability Calculation

3.5.1 Bit Error Probability Calculation for DS-BPSK

The BER for the DS-BPSK system is given by

$$P_e=\Pr(r\le 0/d_0^{(1)}=1) \quad (3.33)$$

Defining $\Lambda=I+n$

From the assumption that MUI and noise is independent of each other. Therefore, we can write the CHF of Λ as

$$\varphi_\Lambda(\omega)=\varphi_I(\omega)\varphi_n(\omega)$$

Where $\varphi_n(\omega)=e^{\frac{-\sigma_n^2\omega^2}{2}}$. Due to the symmetry of MUI and AWGN noise, the bit error probability is given by

$$P_e=\Pr(I+n+A_1\sqrt{E_bN_c}\le 0)$$
$$=1-F_\Lambda(A_1\sqrt{E_bN_c})$$

$$= 1 - \left[\frac{1}{2} + \frac{1}{\pi} \int_0^{\infty} \frac{\sin(A_1 \sqrt{E_b N_c}\,\omega)}{\omega} \right] \phi_{\Lambda}(\omega) d\omega$$

$$= \frac{1}{2} - \frac{1}{\pi} \int_0^{\infty} \frac{\sin(A_1 \sqrt{E_b N_c}\,\omega)}{\omega} \phi_I(\omega) e^{-\frac{\sigma_n^2 \omega^2}{2}} d\omega \qquad (3.34)$$

3.5.2 Bit Error Probability Calculation for DS-PPM

The bit error probability for DS-PPM is given by

$$P_e = \Pr(I + n + S \le 0)$$

$$= 1 - F_{\Lambda}(\pm A_1 \sqrt{E_b N_c})$$

$$= 1 - \left[\frac{1}{2} + \frac{1}{\pi} \int_0^{\infty} \frac{\sin(A_1 \sqrt{E_b N_c}\,\omega)}{\omega} \right] \varphi_I(\omega) d\omega$$

$$= \frac{1}{2} - \frac{1}{\pi} \int_0^{\infty} \frac{\sin(A_1 \sqrt{E_b N_c}\,\omega)}{\omega} \varphi_{I_k}(\omega) e^{-\frac{\sigma_n^2 \omega^2}{2}} d\omega \qquad (3.35)$$

3.6 Simulation Results and Comparisons

In this section, we examine the bit error probability for DS-PPM and DS-BPSK. System parameters used in simulation are listed below.

TABLE-II

VALUE OF THE PRINCIPAL PARAMETERS FOR THE ANALYZED SYSTEM

Parameter	Symbol	Typical Value
Time Normalizing factor	τ_p	0.5 ns
Impulse Width	T_p	0.9 ns
Bit Duration	T_b	14.4/28.8 ns
Modulation Index	δ	0.15 ns
Chip Width	T_c	0.9 ns
Number of users	N_u	8, 16
Number of Chips	N_c	16,32

Fig.3.1 shows the performance of the DS-PPM and DS-BPSK systems with 2^{nd} order Gaussian monocycle assuming 7 asynchronous interferers with time normalizing factor $\tau_p = 0.05\,\text{ns}$. In simulation, we have used Hadamard Walsh code to distinguish each user by assigning a unique spreading sequence to each user. We have already shown in chapter 2, that BPSK outperforms PPM and this validates for DS-BPSK as well. Spreading sequence used is of the length $N_c = 16$.

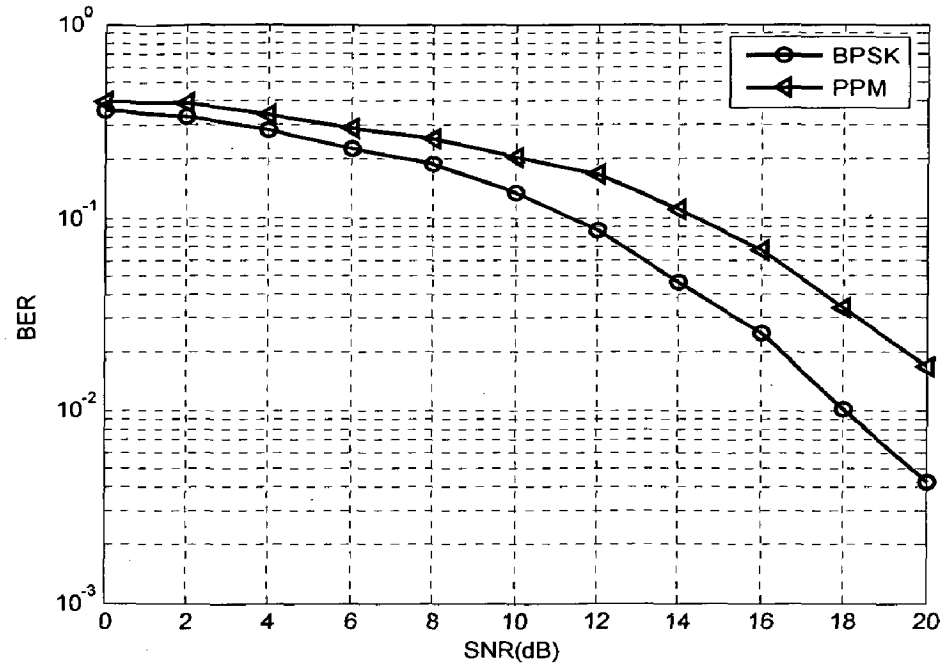

Fig.3.1 Comparison of the DS-PPM and DS-BPSK systems with 7 asynchronous interferers for $\tau_p = 0.05$ ns and $N_c = 16$ for second order Gaussian pulse.

Fig.3.2 indicates the performance using 1^{st} order Gaussian pulse of the DS-BPSK and DS-PPM systems. In order to show the distinct effect of the pulse shape, we have shown the performance comparison of the DS-PPM system for the 1^{st} order and 2^{nd} order Gaussian monocycles in fig 3.3. From fig.3.3, it is clear that system using 2^{nd} order Gaussian pulse performs better than the system using 1^{st} order Gaussian monocycle. Results obtained in direct sequence are in agreement with time hopping results concerning the effect of the pulse shape on the BER performance.

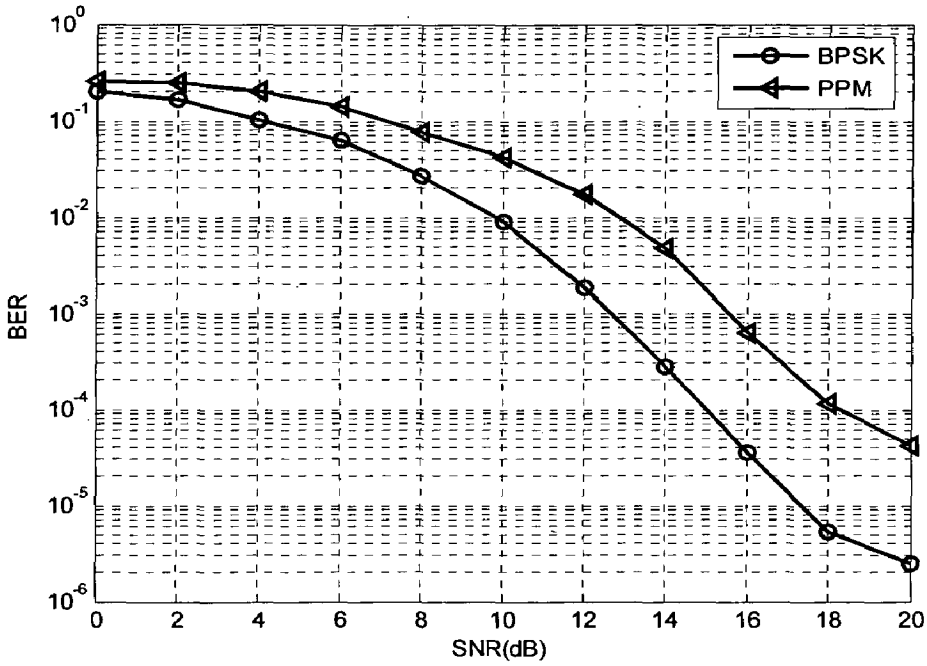

Fig. 3.2.Comparison of the DS-PPM and DS-BPSK systems with 7 asynchronous interferers for $\tau_p = 0.5$ ns and N_c=16 using 1^{st} first order Gaussian pulse.

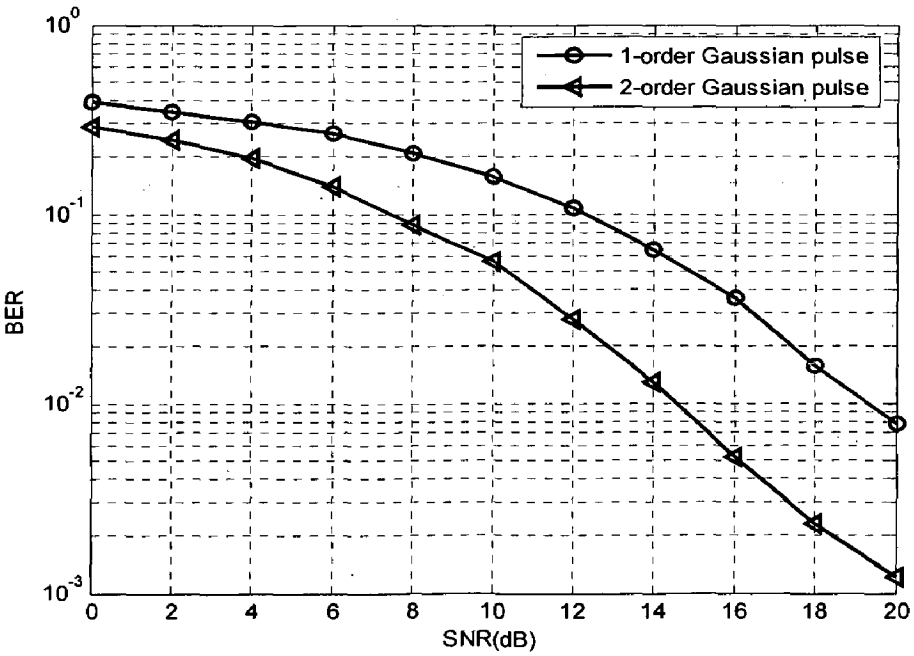

Fig. 3.3. Comparison of the DS-PPM systems using first order and second order Gaussian monocycles with 7 asynchronous interferers for N_c=16 and $\tau_p = 0.5$ ns.

As we increase the length of the spreading sequence, number of pulses representing information bit increases. This increases SNR by $10\log 10\left(\frac{E_b}{N_o}\right)=10\log 10(N_c)+10\log 10\left(\frac{E_p}{N_o}\right)$, where E_p and E_b are pulse and bit energy respectively and N_c is the length of the spreading code. It is evident from the fact that as SNR increases, system performance improves. Fig.3.4 shows the BER curves of the DS-PPM and DS-BPSK systems for $N_c=16$ and $N_c=32$. From the BER curve, it is clear that system having $N_c=32$ outperforms the system having $N_c=16$. In our simulation, we have chosen $\tau_p=0.5\,\text{ns}$ and assuming 7 asynchronous interferers for both DS-PPM and DS-BPSK systems.

Fig.3.5 shows the BER curve of the DS-PPM system for 3 and 7 asynchronous interferers using $\tau_p=0.05\,\text{ns}$ and transmitting pulse is 2^{nd} order Gaussian monocycle shown in fig.2.1.

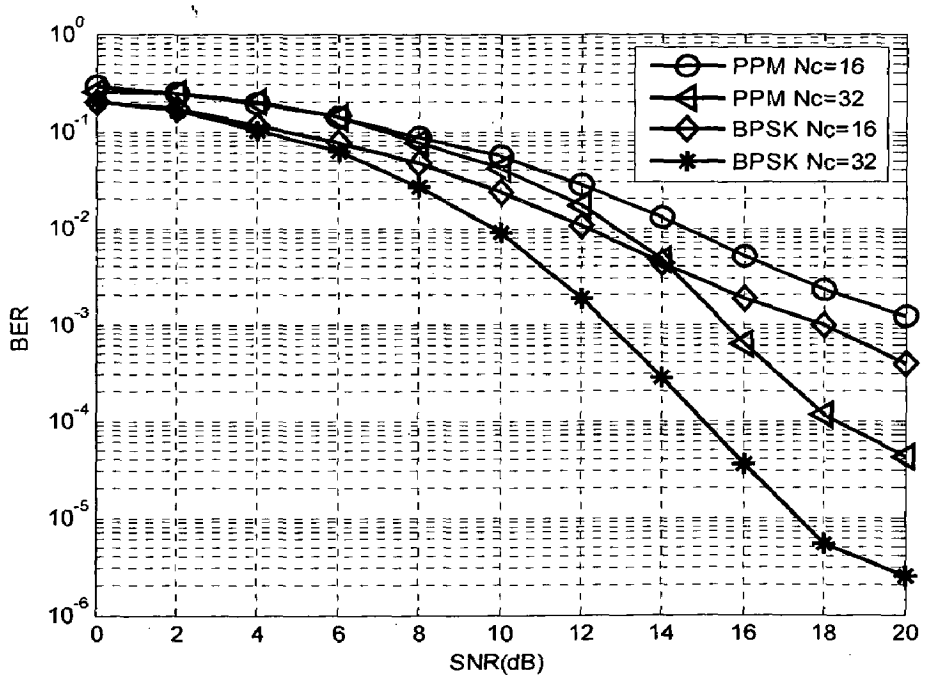

Fig. 3.4 Comparison of the DS-PPM and DS-BPSK systems with 7 asynchronous interferers for N_c=16 and N_c=32 for $\tau_p=0.5$ ns.

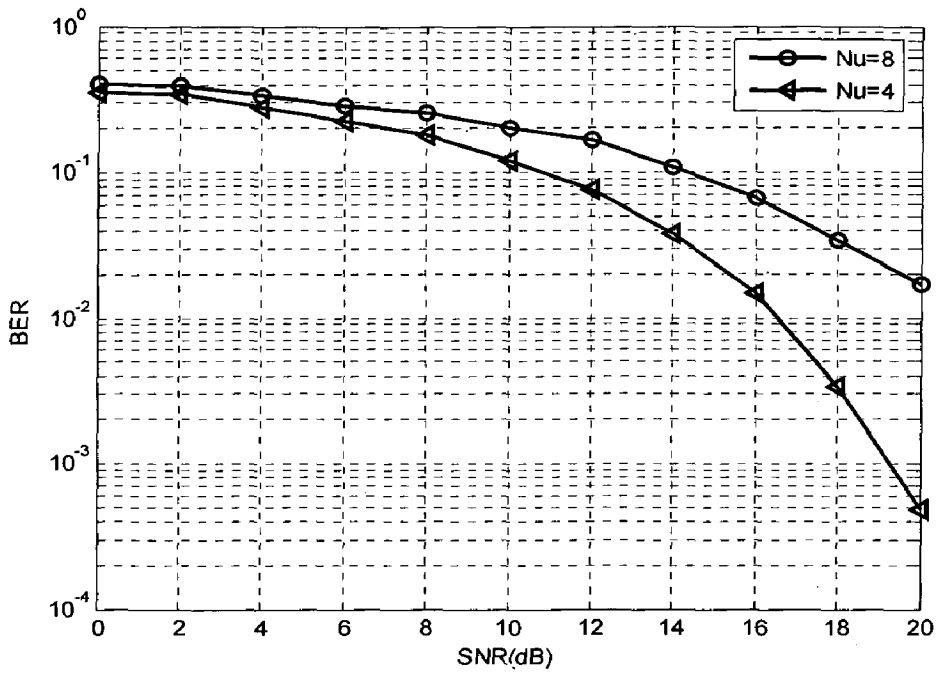

Fig.3.5 Comparison of the DS-PPM system for 7 and 3 asynchronous interferers for $\tau_p = 0.05$ ns and N_c=16 .

Results obtained for time normalizing factor are interesting. In chapter 2, we have shown that TH-PPM system with $\tau_p = 0.2$ ns outperforms the system with $\tau_p = 0.05$ ns. Here scenario is different, fig.3.6 shows that, system with $\tau_p = 0.3$ ns performs better than the system with $\tau_p = 0.2$ ns. In fig.3.7, It is shown that DS-PPM system with $\tau_p = 0.4$ ns performs better than the DS-PPM system with $\tau_p = 0.6$ ns. Fig.3.6 and fig.3.7 shows that the BER is not monotonically increasing or decreasing with τ_p. From equation (3.21), we can say that BER is a function of $\tilde{R}(0) = 1 - R(-\delta)$.

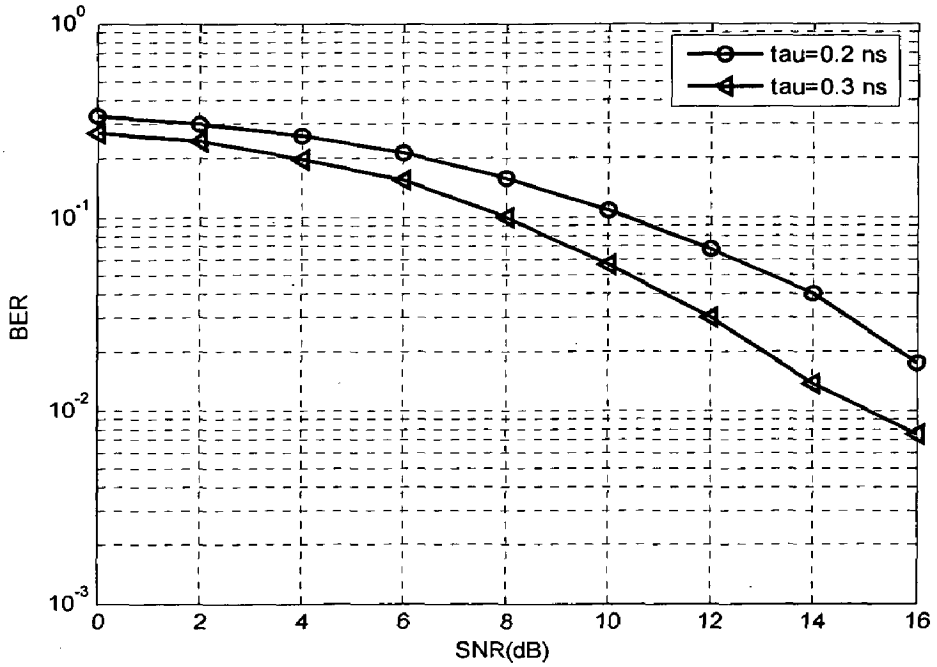

Fig. 3.6 Average BER of the DS-PPM system versus SNR for $\tau_p = 0.2$ ns and $\tau_p = 0.3$ assuming 7 asynchronous interferers with N_c=16.

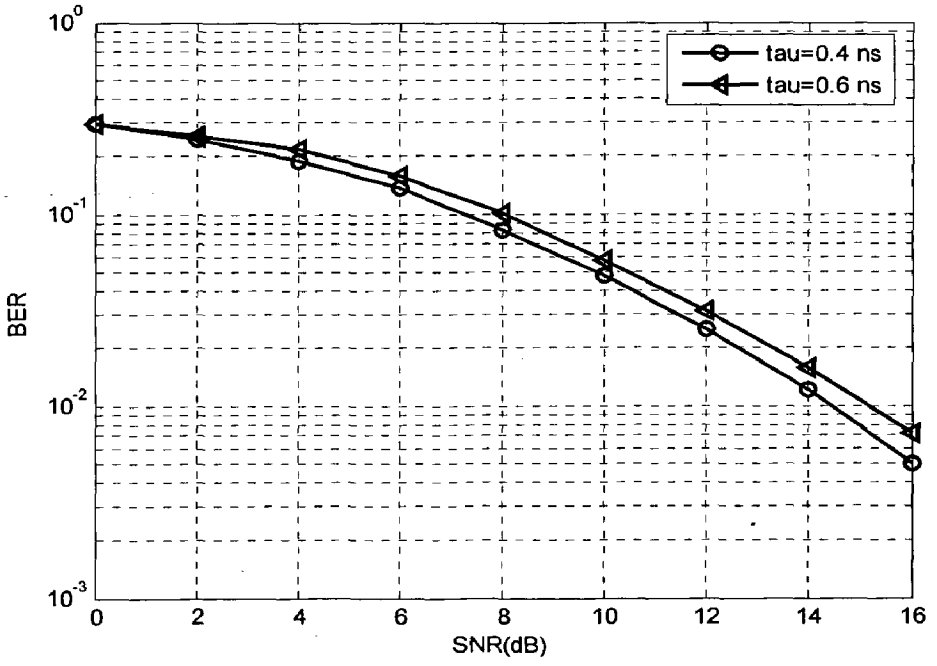

Fig. 3.7 Average BER of the DS-PPM system versus SNR for $\tau_p = 0.4$ ns and $\tau_p = 0.6$ assuming 7 asynchronous interferers with N_c=16.

CONCLUSION

In chapter 2 and 3, we have calculated the probability of error for TH-PPM, TH-BPSK, DS-PPM and DS-BPSK systems. From [10], [11], [13], [14] and [21], it is shown that results obtained using characteristic function method is more accurate than the Gaussian approximation of the multi access interference.

Our comparison results of the performance of time-hopping and direct-sequence UWB systems in the presence of multi access interference, as measured by the probability of bit error, showed that BPSK systems outperforms the PPM systems for all values of SNR.

In addition, our simulation results show that system using second order pulse performs better than the first order pulse used system. So pulse selection in UWB is important from the BER point of view. Long spreading codes can be used for performance. Different values of time normalizing factor gives different bit error probability for different values. Finally, more active users creates more interference and lead to system BER performance degradation.

REFERENCES

1) G. R. Aiello and G. D. Rogerson, "Utra-Wideband Wireless Systems," *IEEE Microwave Magazine,* pp. 36-47, June 2003.
2) W. Zhuang, X. Shen and Qi Bi, "Ultra-Wideband Wireless Communications," *Wireless Communications and Mobile Computing,,* pp. 663-685, 2003.
3) L. Yang and G. B. Giannakis, "Ultra-Wideban Communications," *IEEE Signal Processing Magzine,* pp. 26-54, Nov 2004.
4) M. Ghavami, L. B. Michael and R. Kohno, Ultra-Wideband Signal and Systems in Communication Engineering, John Wiley and Sons, Ltd. 2004.
5) G. Durisi and S. Benedetto, "Performance Evaluation of TH-PPM UWB Systems in the Presence of Multiuser Interference," *IEEE Communications Letters,* vol. 7, no. 5, pp. 224-226, May 2003 .
6) V. S. Somayanulu, "Multiple Acess Performance in UWB Ststens using Time Hopping vs. Direct Sequence Spreading,", *Wireless Communications and Networking Conference, 2002.WCNC2002.2002 IEEE,* vol. 2, pp. 522–525, Mar 2002.
7) G. Durisi and S. Benedetto, "Performance Evaluation and Comparison of Different Modulation Schemes for UWB Multiaccess Systems," *Communications, 2003.ICC'03.IEEE International Conference,* vol. 3, pp. 2187-2191, May 2003.
8) R. A. Scholtz, "Multi Aceess with Time-Hopping Impulse Modulation," *Military Communications Conference, 1993. MILCOM'93. Conference record. 'Communications on the Move'. IEEE,* vol. 2, pp. 447–450, Oct 1993.
9) Bo Hu and Norman C. Beaulieu, "Precise Bit Error Rate of TH-PPM UWB Systems in the Presence of Multiple Access Interference," *Ultra Wideband Systems and Technologies, 2003 IEEE Conference*, pp. 106–110, Nov 2003.
10) Bo Hu and Norman C. Beaulieu, "Accurate Evaluation of Multiple Access Performance in Time-Hopping UWB Systems," *Communications, 2004 IEEE International Conference*, vol. 1, pp. 300–305, June 2004.

11) Bo Hu and Norman C. Beaulieu, "Accurate Evaluation of Time-Hopping and Direct-Sequence UWB Systems in Multi-User Interference," *IEEE Transactions on Communications*, vol. 53, no. 6, pp. 1053–1062, June 2005.

12) M. Z. Win and R. A. Scholtz, "Ultra-Wide Bandwidth Time-Hopping Spread-Spectrum Impulse Radio for Wireless Multiple-Access Communications," *IEEE Transactions on Communications*, vol. 48, no. 4, pp. 679–691, April 2000.

13) M. Sabattini, E. Masry and L. B. Milstein, "A Non-Gaussian Approach to the Performance Analysis of UWB TH-BPPM Systems," *Ultra Wideband Systems and Technologies, 2003 IEEE Conference*, pp. 52–55, Nov.2003.

14) K. A. Hamdi and X. Gu, "On the Validity of the Gaussian Approximation for Performance Analysis of TH-CDMA/OOK Impulse Radio Networks," *Vehicular Technology Conference, 2003.VTC2003-Spring. The 57th IEEE Semiannual*, vol. 4, pp. 2211–2215, April 2003.

15) C. Muller, S. Zeisberg and A. Finger, "Spreading Properties of Time Hopping Codes in Ultra Wideband Systems," *IEEE 7th Int. Symp. on Spread-Spectrum Tech .& Appl., Prague, Crech Republic*, pp. 64–67, Sept. 2002.

16) A. J. Viterbi, "Spread Spectrum Communications: Myth and Realities," *IEEE Communicaions Magzine*, vol. 40, issue 5, pp. 34–41, May 2002.

17) N. Boubaker and K. B. Letaief, "Performance Analysis of DS-UWB Multiple Access Under Imperfect Power Control," *IEEE Transactions on Communications*, vol. 52, no. 9, pp. 1459–1463, Sept. 2004.

18) N. Boubaker and K. B. Letaief, "Ultra Wideband DSSS for Multiple Access Communications Using Antipodal Signaling," *Communications, 2003, ICC'03. IEEE International Conference*, vol. 3, pp. 2197–2201, May 2003.

19) B. M. Sadler and A. Swami, "On the Performance of Episodic UWB and Direct-Sequence Communication Systems," *IEEE Transactions on Wireless Communications*, vol. 3, no. 6, pp. 2246–2255, Nov. 2004.

20) B. M. Sadler and A. Swami, "On the Performance of UWB and DS-Spread Spectrum Communication Systems," *IEEE Conference on Ultra Wideband Systems and Technologies*, pp. 289–292, 2002.

21) W. Cao, A. Nallanathan, B. Kannan and C. C. Chai, "Exact BER Analysis of DS PPM UWB Multiple Access System Under Imperfect Power Control," *Military Communications Conference, 2005. MILCOM 2005. IEEE*, vol. 2, pp. 977–982, Oct. 2005.

22) D. In Kim, "Combined Binary Pulse Position Modulation/Biorthogonal Modulation for Direct-Sequence Code Division Multiple Access," *IEEE Transactions on Wireless Communications*, vol. 47, no. 1, pp. 22–26, Jan. 1999.

23) I. D. Lee and H. P. Stern, "Direct Sequence CDMA Design for Mobile Cellular Systems," *System Theory, 1994. Proceedings of the 26th Southeastern Symposium*, pp. 585–589, Mar. 1994.

24) H. Chen, W. Li, A. Gulliver and H. Zhang, "DS-PPM Ultra-Wideband Communications with BCH Coding," *Communications, Computers and Signal Processing, 2005. PACRIM. 2005 IEEE Pacific Rim Conference*, pp. 17–20, Aug. 2005.

25) N. V. Yen, "Performance of DS UWB with MUD Schemes," *IJCSNS International Journal of Computer Science and Network Security*, vol. 7, no. 2, pp. 176–180, Feb. 2007.